



Numerical 3D modeling of burial and temperature history, source rock maturity, and hydrocarbon generation in the onshore northeastern Netherlands

Sebastian Amberg^{1,2} · Stefan Back² · Victoria Sachse¹ · Ralf Littke¹

Received: 27 January 2021 / Accepted: 28 January 2022 / Published online: 22 February 2022
© The Author(s) 2022

Abstract

Numerical 3D basin modeling is used to reconstruct the burial and temperature histories in onshore northeastern Netherlands, incorporating the four main geological structural elements Groningen Platform, Lauwerszee Trough, Friesland Platform, and Lower Saxony Basin. The structural framework is based on recently published open access depth surface data; public temperature and vitrinite reflectance data from 28 wells are used to evaluate burial and temperature histories. Four modeled burial histories and the maturity evolution of the structural elements are presented. The hydrocarbon generation in major source rock intervals in the Carboniferous, Jurassic, and Cretaceous is simulated using recently published kinetic and literature data. Modeling results indicate highest present-day temperatures and maturities of the Paleozoic sedimentary succession in the Lauwerszee Trough and the Lower Saxony Basin, where the deepest burial occurred. Two major phases of deep burial and subsequent uplift occurred in Carboniferous to Permian times and from the Triassic to the Jurassic. Both intervals strongly influenced the maturation and transformation of kerogen from Paleozoic source rocks. The highest modeled maturities of the Mesozoic groups are observed in depressions between salt diapirs in the Lower Saxony Basin. Out of the two major source rock intervals within the Mesozoic, the Cretaceous Wealden Shale generated hydrocarbons from Late Cretaceous times.

Keywords Sedimentary basin dynamics · Basin and petroleum system modeling · Vitrinite reflectance · Seismic interpretation · Central European Basin System · Northeastern Netherlands

Introduction

The northeastern part of the onshore Netherlands hosts some of the most important hydrocarbon accumulations in continental Europe including the giant Groningen gas field. For a better understanding of the formation mechanisms of these hydrocarbon accumulations, it is essential to reconstruct the burial history and maturity evolution of the sedimentary succession and the timing of hydrocarbon generation from Paleozoic and Mesozoic source rocks. This can be achieved

using numerical models to reconstruct the thermal evolution of a sedimentary basin, which depends to a large extent on the subsidence and paleo heat flow history. A few large-scale numerical models were published in recent years that studied the structural history, the thermal evolution, and the petroleum systems of the Netherlands and adjacent areas. Nelskamp (2011) published various numerical 1D basin and petroleum systems models (BPSM) and a 2D model along a cross-section across the Netherlands extending from the London Brabant Massif in the southwest to the Dutch Lower Saxony Basin in the northeast. For calibration of these models, constant heat flow values of 55 and 65 mW/m² and up to five erosional events were applied (Paleozoic and younger; Nelskamp 2011). Large-scale 3D models covering even larger areas of the Central European Basin System (CEBS) were published, e.g. by Schroot et al. (2006), Uffmann and Littke (2011), Bruns et al. (2013), Bruns et al. (2016), Mohnhoff et al. (2016) and Sachse and Littke (2018). A 3D petroleum system model of the North German Basin was created by Uffmann and Littke (2011), using various

✉ Sebastian Amberg
sebastian.amberg@emr.rwth-aachen.de

¹ Institute of Geology and Geochemistry of Petroleum and Coal, Energy and Mineral Resources (EMR), RWTH Aachen University, Lochnerstr. 4-20, 52054 Aachen, Germany

² Geological Institute, Energy and Mineral Resources (EMR), RWTH Aachen University, Wüllnerstr. 2, 52052 Aachen, Germany

paleo heat flow trends that included elevated heat flow values related to extensional tectonics in Early Permian times and in Jurassic times for the rift basins. Bruns et al. (2016) used an additional heat flow scenario based on the approach by Van Wees et al. (2000) and Van Wees et al. (2009), taking into account the thermal effect of rapid inversion and uplift in their large-scale 3D model covering Northern Germany and the Netherlands; both scenarios showed differences in the amount of eroded sediments needed for calibration.

This study aims to complement previous studies and provide a detailed regional overview of the burial, temperature, and maturity history of important structural elements of the NE Netherlands as well as the present-day temperature and maturity of the sedimentary succession. The petroleum systems within the study area were analyzed and the amount and timing of petroleum generation of Paleozoic and Mesozoic source rocks were assessed in detail using 3D basin modeling. The different burial and heat flow histories of basin and platform areas are compared and analyzed. Seismic reflection data were used to identify five unconformities related to major erosion events; these data were implemented in the 3D petroleum systems model. 3D seismic interpretation and basin modeling approaches were combined with depth maps from the Digital Geological Model-deep v5 (TNO-GSN 2020a), the SCAN 2D project (TNO-GSN 2020b), and Maystrenko et al. (2020); stratigraphic and well information from the DINOloket database (TNO-GSN 2020c), new kinetic data of two major source rocks (Carboniferous, Wealden) in the area (Froidl et al. 2020a, b); and information from previous studies on the regional geology (TNO-NITG 2004; Schroot et al. 2006; Nelskamp 2011; Groetsch et al. 2011; Bouroullec et al. 2019). A 3D model was built integrating numerical 1D simulations at 28 well locations, including distinct erosional intervals interpreted from truncation surfaces on seismic-reflection and well data.

Geology of the study area

The subsurface of the northeast of the Netherlands was influenced by major tectonic events from Paleozoic times until the present-day, including the formation and later breaking apart of the super continent Pangea as well as the Alpine collision (De Jager 2003). The Central European Basin System (CEBS), a large-scale structure comprising the Northern and Southern Permian Basin, is superimposed on the Westphalian foreland basin (Maystrenko et al. 2008).

The studied area covers the following regional structural elements (Fig. 1a): Lower Saxony Basin (LSB), Friesland Platform (FP), Dalfsen High (DH), Lauwerszee Trough (LT), and the Groningen Platform (GP), which are located at the southern margin of the Southern Permian Basin (SPB) (Kombrink et al. 2012). These structures were formed during

Mesozoic Kimmerian rifting (De Jager 2007; Kley et al. 2008). The underlying NW–SE structural trend originates from the Caledonian orogeny (Silurian to Devonian; De Jager 2003). According to the definition of Duin et al. (2006) and Kombrink et al. (2012), platforms and highs in the Netherlands are in contrast to basins or troughs characterized by significant Late Jurassic erosion down to Carboniferous or Triassic units (Fig. 1b). Salt occurs widespread throughout the study area in salt pillows, salt walls, and salt domes (Fig. 1b). Salt bodies often have elongated shapes with a predominant N–S orientation, are mostly related to sub-salt faults and intersections of faults, and formed during the disintegration of the SPB in the Triassic to Jurassic (Geluk et al. 2007; Scheck-Wenderoth et al. 2008).

During the Early Carboniferous, sedimentation was characterized by carbonate deposition, whereas in the Namurian, an increasing influx of siliciclastic material came from the Fennoscandian Shield and Variscides in the north and south, respectively (Fig. 2; Collinson 2005; Kombrink 2008). Bituminous shales of the Geverik Member, which might act as source rocks in parts of the Netherlands, were deposited in the Early Namurian (Schroot et al. 2006).

A coastal plain with swamps in a tropical climate prevailed during the Westphalian leading to the deposition of peat and siliciclastic sediments in rivers and deltas (Fig. 2; Littke 1985; Maystrenko et al. 2008). Sediments of Namurian and Westphalian age belong in the study area to the Limburg Group (Fig. 2) and reach a thickness of up to 5.5 km in the Netherlands (Van Buggenum and den Hartog Jager 2007; Nelskamp 2011). Late Westphalian and Stephanian deposits are only preserved in the Lower Saxony Basin (Fig. 2; Van Buggenum and den Hartog Jager 2007; Groetsch et al. 2011).

Late Carboniferous and Early Permian thermal uplift led to deep erosion accompanied by intrusive and extrusive magmatism (De Jager 2007). Transtensional movements formed pull-apart basins with restricted sedimentation of fluvial and aeolian sediments of the Rotliegend Group (McCann et al. 2006; Bachmann et al. 2008; Mijnlief and Geluk 2011; Strozyk et al. 2017). Extension, regional thermal subsidence, and a transgression and subsequent flooding of low-lying Rotliegend basins introduced marine conditions in the area of the Netherlands at the base of the Zechstein. A later incremental marine regression led to the deposition of the Zechstein salt sequences, out of which five evaporitic cycles are present in the Netherlands with an upward decreasing marine influence that show a more playa-type depositional setting (Bachmann et al. 2008; Strozyk et al. 2017).

Four extensional tectonic phases, the Hardegsen, Early Kimmerian, Mid Kimmerian, and Late Kimmerian are related to the break-up of Pangea and the subdivision of the SPB into several fault-bounded sub-basins between

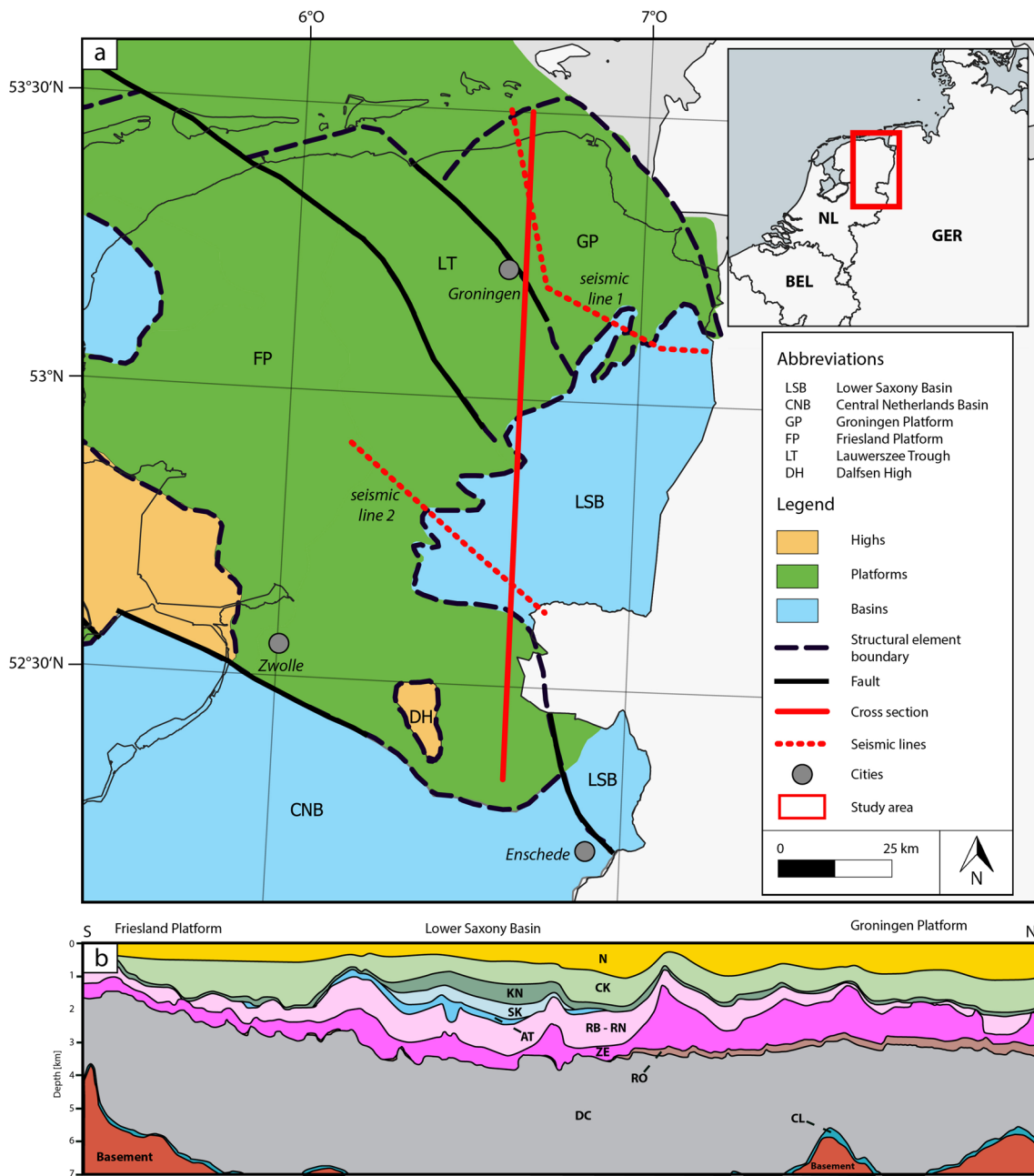


Fig. 1 **a** Major structural elements in the northeastern part of the onshore Netherlands including main platforms, highs, troughs and basins and location of the cross section and position of the study area in Central Europe (modified from Kombrink et al. 2012). Location of interpreted seismic lines is indicated with dotted red lines. **b** N–S cross section with major structural elements such as the platforms, the basin and the general stratigraphy, and elevated salt structures

across the study area based on DGM-Deep v5 and SCAN2D depth maps (TNO-GSN 2020a, b) (*N* North Sea Group, *CK* Chalk Group, *KN* Rijnland Group, *SK* Niedersachsen Group, *AT* Altena Group, *RB–RN* Upper and Lower Germanic Trias Group, *ZE* Zechstein Group, *RO* Rotliegend Group, *DC* Limburg Group, *CL* Carboniferous Limestone Group, *Basement* Pre-Carboniferous basement). Location of the cross section illustrated in **a** (solid red line)

the Triassic and the Cretaceous (Geluk 2007; Stollhofen et al. 2008; Nelskamp 2011). During two of these extensional phases, Hardeggen and Early Kimmerian, Zechstein salt became mobile (Geluk 2007; Strozyk et al. 2017). The Variscan mountain belt in the south acted as the main source of clastic sediments until the Middle Triassic (Geluk 2007).

Late Triassic coastal-plain to marine clastic sediments, sourced by an uplift of Fennoscandia to the north, are in the Netherlands only preserved in subsequently formed Jurassic rift basins (De Jager 2007; Geluk 2007).

A marine transgression resulted in the deposition of fine-grained clastic sediments of the Altena Group in the Early

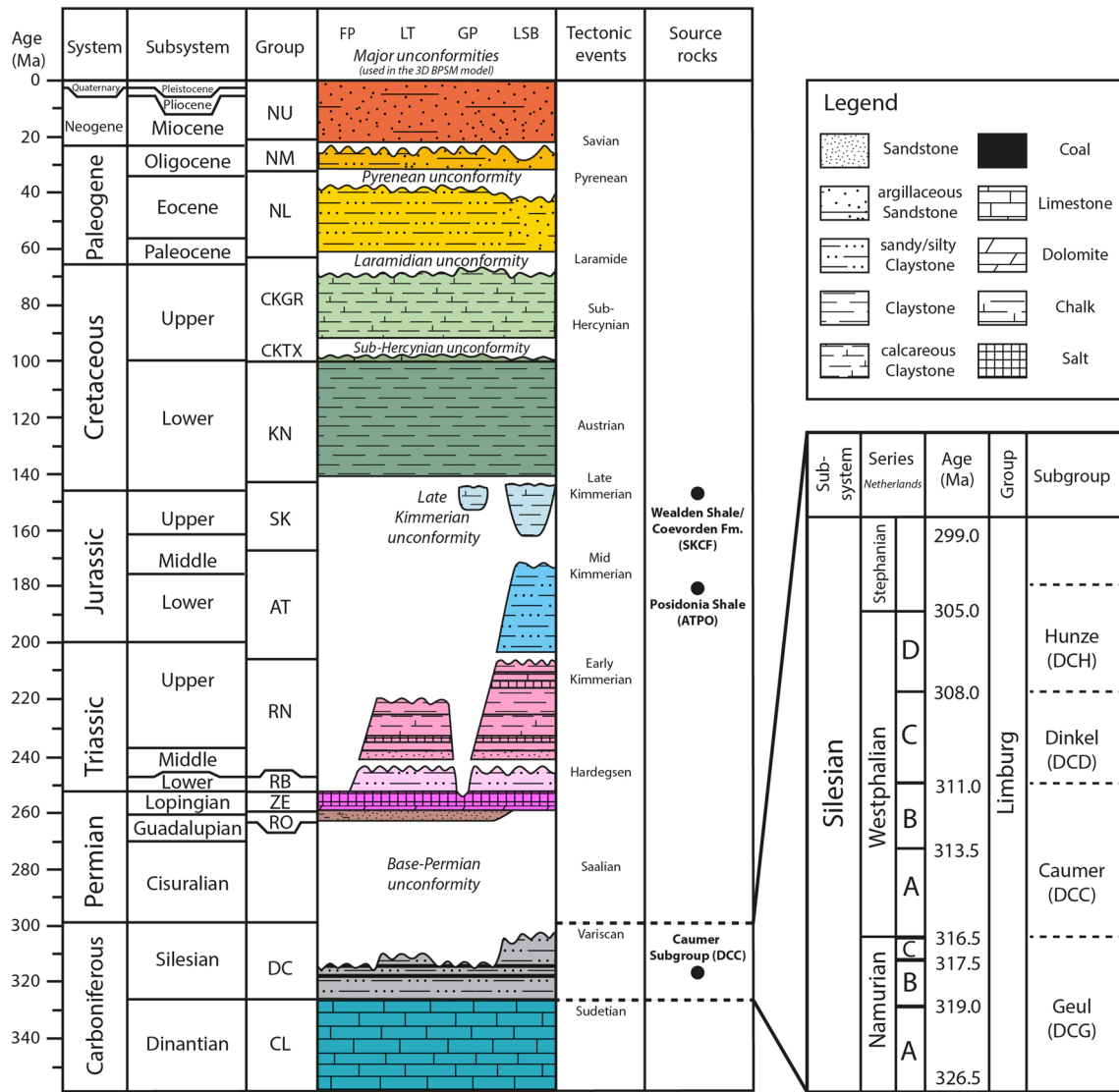


Fig. 2 Chronostratigraphic chart with major tectonic events, lithologies and presence of main sedimentary units within the study area according to the general stratigraphic nomenclature of the Netherlands and stratigraphic subdivision of the Carboniferous in the north-western Netherlands (Nam and RGD 1980; Van Adrichem Boogaert and Kouwe 1994; TNO-NITG 2004; Van Buggenum and den Hartog Jager 2007; Wong et al. 2007; TNO-GSN 2020c). Unconformities identified on seismic reflection data and implemented in the 3D model are highlighted. Major source rock intervals are listed in a separate column.

Stratigraphic subdivision of the Silesian in the Netherlands modified from van Buggenum and den Hartog Jager (2007). NU Upper North Sea Group, NM Middle North Sea Group, NL Lower North Sea Group, CK Chalk Group (CKGR Ommelanden Formation, CKTX Texel Formation); KN Rijnland Group, SK Niedersachsen Group, AT Altena Group, RB Upper Germanic Trias Group, RN Lower Germanic Trias Group, ZE Zechstein Group, RO Rotliegend Group, DC Limburg Group, CL Carboniferous Limestone Group

Jurassic (De Jager 2007; Wong 2007). An organic-rich shale that acts as one of the major source rocks in the CEBS, the Posidonia Shale, was deposited in Toarcian times (Song et al. 2017). In the Late Jurassic, extension related to the crustal separation in the Central Atlantic led to the formation of graben structures such as the Lower Saxony Basin with restricted syn-rift sedimentation and the uplift of adjacent graben shoulders (e.g. Groningen Platform) that were partly eroded and acted as the main clastic sediment source for the

adjacent basins (Wong 2007; Bachmann et al. 2008). This configuration of basins and highs persisted into the Early Cretaceous. Upper Jurassic sedimentation was primarily limited to the basins, on structural highs an unconformity with an estimated hiatus of locally more than 20 Ma can be observed, referred to as the Mid Kimmerian Unconformity (Wong 2007). The Late Kimmerian Unconformity, which can be traced over the whole study area, is interpreted to record a sea-level lowstand in the Early Cretaceous (Rawson

and Riley 1982; De Jager 2007). According to Groetsch et al. (2011), it remains unclear to what extent the Groningen area acted as a high during the Kimmerian extensional phase as Jurassic sediments are absent.

In the Early Cretaceous, extensional tectonics ceased. Regional subsidence accompanied by a major transgression initiated the deposition of sediments, at first, restricted to the basins and by Aptian times region-wide on pre-existing highs and platforms (Herngreen and Wong 2007; Groetsch et al. 2011). Deepwater carbonates of the Chalk Group were deposited throughout the Late Cretaceous (Herngreen and Wong 2007). The convergence of Europe, Africa and Iberia during the Late Cretaceous marked the beginning of the Alpine orogeny (Kley 2018). The Alpine orogeny and contemporaneous extension in the Atlantic Ocean initiated inversion of Mesozoic extensional basins in several pulses, including the Sub-Hercynian (Late Cretaceous), the Laramide (Paleocene), the Pyrenean (Eocene), and the Savian in the Oligocene (De Jager 2007; Bachmann et al. 2008). The presence or absence of Zechstein salt had a strong influence on how the inversion affected different parts of the Netherlands (De Jager 2007).

During the Cenozoic, predominantly siliciclastic sediments were deposited and several unconformities occur, attributed to sea-level changes or tectonic movements (Wong et al. 2007; Nelskamp 2011). The Quaternary is characterized by a strong increase in sedimentation rates (De Gans 2007). The occurrence of glacial and interglacial periods lead to a large variety of depositional systems (Nelskamp 2011). During two glacial periods, the Elsterian and Saalian, ice sheets were advancing onto the Netherlands (Ehlers et al. 2018).

Petroleum systems

There is a variety of active petroleum systems in the CEBS, out of which the Paleozoic and Mesozoic systems contribute most to the discovered hydrocarbons volumes in the CEBS (Maystrenko et al. 2008; Doornenbal et al. 2019). Major hydrocarbon discoveries in the NE Netherlands are the giant Groningen gas field (largest gas field in the CEBS) and the Schoonebeek oil field at the Dutch-German border in Drenthe (Geluk et al. 2009; Groetsch et al. 2011).

Coal-bearing Late Carboniferous sediments, assigned to the Limburg Group, are the main source rocks for the Paleozoic petroleum system (Fig. 2). The amount of coal varies in each subgroup of the Limburg Group, but is proposed to be highest in the Caumer Subgroup; it ranges overall from 0.1 to 5% (van Buggenum and den Hartog Jager 2007; Nelskamp 2011) and is thus somewhat lower than in the Ruhr Basin further south (Scheidt and Littke 1989), where this sequence is well exposed. Marine basal Namurian organic-rich shales are discussed to have contributed to high nitrogen

contents (Krooss et al. 2008; Groetsch et al. 2011). Nitrogen contents in natural gas accumulations vary across the CEBS with regional trends depending on the maximum burial of Carboniferous source rocks (Maystrenko et al. 2008). In the northern and eastern part of the CEBS, nitrogen contents of up to 90% are found in natural gas accumulations (Krooss et al. 2008). The bulk of hydrocarbons discovered in the Netherlands originates from this Paleozoic petroleum system. The giant Groningen field, which accounts for two-thirds of recoverable natural gas reserves in the Netherlands, is produced from Rotliegend sandstones, mainly sourced by Carboniferous coals and dispersed kerogen (Jasper et al. 2009); the seal is formed by Zechstein salt (De Jager and Geluk 2007; Groetsch et al. 2011). This gas play is by far the most important one, but additional gas accumulations are found in Carboniferous and Triassic sandstones, Zechstein carbonates, and fluviomarine Jurassic and Cretaceous reservoirs (Rondeel et al. 1996).

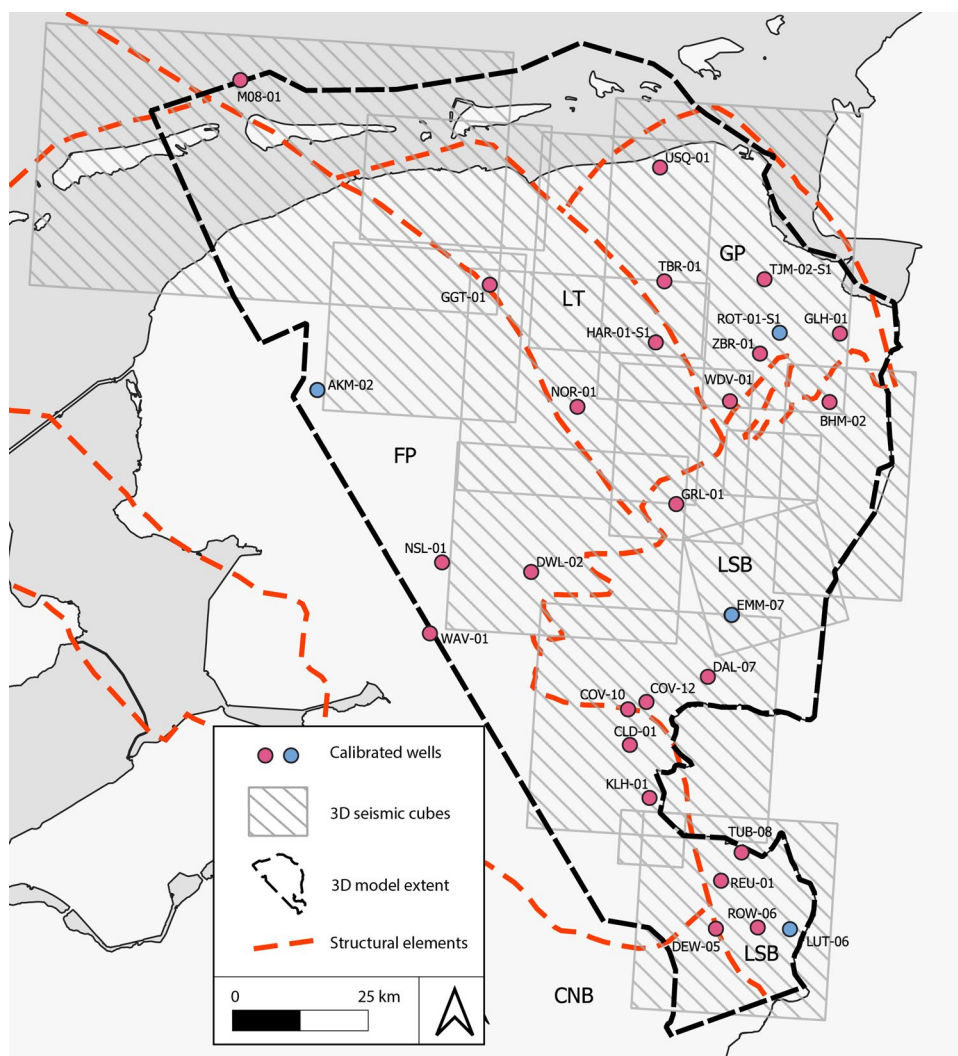
In contrast to predominantly gas-bearing source rocks of the Paleozoic, the most important Mesozoic source rocks in the NE Netherlands are oil-prone (De Jager and Geluk 2007). This includes the marine Toarcian Posidonia shale, which, in the study area, only occurs in the Lower Saxony Basin at the border to Germany and the Beriasian lacustrine Coevorden Formation, known as the Wealden Shale (Littke et al. 1991; Di Primio et al. 2008; Rippen et al. 2013; Bruns et al. 2016; Froidl et al. 2020b). Oil accumulations are limited to Late Jurassic rift basins, in which e.g. the Wealden shale is discussed to have sourced the large Schoonebeek oil field (De Jager and Geluk 2007; Nelskamp 2011).

Methods

Input

The 3D basin model (extent on Fig. 3) is based on 13 depth maps from the Digital Geological Model-deep v5 (DGM-deep), which is a regional subsurface model of the Netherlands, released in January 2020 (TNO-GSN 2020a). It has a spatial resolution of 250 × 250 m and reaches down to the base of the Upper Carboniferous Caumer Subgroup. Two additional depth maps with a grid resolution of 250 × 250 m from the SCAN 2D project (TNO-GSN 2020b), which aims to study the geothermal heat potential of the Carboniferous Limestone Group (Dinantian) in the Netherlands released by TNO in November 2019, were used to complement the stratigraphic succession down to the base of the Lower Carboniferous. Nine thickness maps of the main Paleozoic and Mesozoic sedimentary units were created from the geological subsurface model DGM Deep v5 (TNO-GSN 2020a) and the SCAN 2D project (TNO-GSN 2020b) and are illustrated in Fig. 4. A surface representing the top crystalline basement

Fig. 3 Extent of the 3D model including main structural elements, location of 3D seismic and wells with available temperature and vitrinite reflectance data used for the calibration of the model. Wells marked in blue color are used as representative wells for the burial history of main structures



from Maystrenko et al. (2020) with a horizontal grid spacing of 4 km was added to distinguish pre-Carboniferous sediments from the crystalline basement and account for correct radiogenic heat production in the deep subsurface (Scheck-Wenderoth and Maystrenko 2013). Well data used in this project, including stratigraphic information, well logs, temperature, vitrinite and pressure measurements, were accessed from TNO's public NLOG (<http://www.nlog.nl>) and DINOLoket database (<http://www.dinoloket.nl>; TNO-GSN 2020c). Out of this database, 28 wells were used to calibrate the 3D model with respect to its burial and thermal history (Fig. 3).

Seismic-reflection data

Fifteen 3D seismic-reflection volumes in the study area were provided by the Nederlandse Aardolie Maatschappij b.v. (NAM) and TNO (Fig. 3). Key marker horizons, seismic units and unconformities were identified based on seismic

reflector configurations. Unconformities indicating major erosion phases were used in the modeling workflow.

PetroMod

The 1D models as well as the 3D basin model were built using Schlumberger PetroMod® 2019. The modeling principles and the workflow in the software are described in detail in Hantschel and Kauerauf (2009) and Peters et al. (2017). A basin and petroleum systems model is a deterministic forward model calculating the geological development of an area as well as rock and fluid properties forward in time (Hantschel and Kauerauf 2009). It is built using input data such as present-day geological models, paleo geometries, thermal boundary conditions and is calibrated to measured parameters of a study area (Peters et al. 2017). The study area is located in the northeast of the Netherlands, extending from the Dutch Frisian Islands in the northwest to the Dutch–German border near Enschede in the east, covering

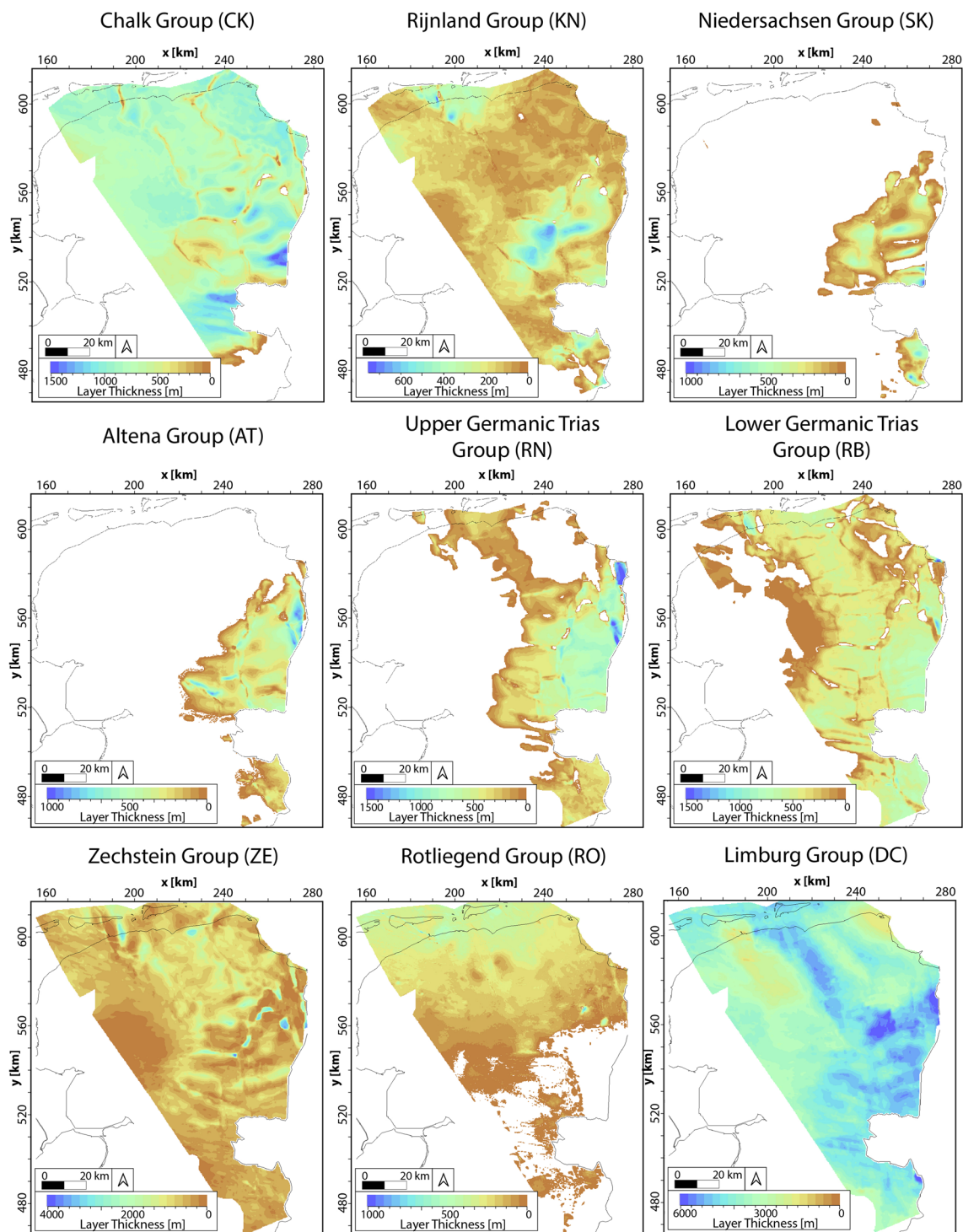


Fig. 4 Present-day thickness maps of main Paleozoic and Mesozoic units (Fig. 2); Triassic: Lower and Upper Germanic Trias Groups; Jurassic: Altena and Niedersachsen Group; Cretaceous: Rijnland and Chalk Group. Triassic groups are missing in parts of the plat-

forms, while Jurassic groups are just present in the basins; Permian: Zechstein and Rotliegend Group; Carboniferous (Silesian): Limburg Group

approximately 10,000 km² (Fig. 3). Thereby, the 3D models maximum extent is around 150 km from north to south and 100 km from east to west. Cells have a size of 250 × 250 m

and the grid resolution of the 3D model is 1072 by 1280 cells. The 3D model comprises 21 stratigraphic units from the crystalline basement to the Upper North Sea Group

according to the general stratigraphic nomenclature of the Netherlands (NAM and RGD 1980; Van Adrichem Boogaert and Kouwe 1994; TNO-GSN 2020c). Lithologies have been combined from TNO-NITG (2004), Wong et al. (2007), Nelskamp (2011) and TNO-GSN (2020c) and were assigned to the model as shown in Table 1. Some layers, representing major lithostratigraphic units such as the Paleogene to Neogene North Sea Group (NS), the Cretaceous Chalk Group (CK), and the Carboniferous Limburg Group (DC), were further subdivided and refined to implement source rock intervals and major erosions using well top markers across the study area. Only major erosion events were implemented into the 3D model, as shown in Table 1. The following five events were identified on seismic and well data and assigned to the model representing major regional erosions according to De Jager (2007): Base-Permian (Permian); Late Kimmerian (Triassic–Jurassic); Sub-Hercynian (Cretaceous); Laramide (Paleogene); Pyrenean (Paleogene). Erosion maps are based on the interpretation of the 1D calibration results using vitrinite reflectance. Erosion amounts at well locations

were spatially interpolated using the built-in Laplace interpolation method in PetroMod. Due to the widespread presence of Zechstein Salt within the study area, the salt facies piercing tool in PetroMod was used to approximate the effect of salt diapirism on the stratigraphic succession. Phases of major salt diapirism were set to the Late Triassic and the Jurassic related to extensional tectonics according to Geluk et al. (2007), Strozyk et al. (2014) and Strozyk et al. (2017).

Boundary conditions

The paleo basal heat flow as the lower thermal boundary condition was set to 60 mW/m², close to the average heat flow in continental crust (Allen and Allen 2013) and close to the average present-day heat flow in central Europe (Hurter and Haenel 2002). Higher heat flows of up to 90 mW/m² (Uffmann and Littke 2011) were applied for the Permian, when intense volcanism took place in the area and for the Late Jurassic to earliest Cretaceous phase of rifting in the Lower Saxony Basin (up to 80 mW/m²; see Adriasola Munoz

Table 1 General input data for modelling of burial, temperature and erosion history of the 3D model

Layer	Age (Ma)	Event type	Main lithology (fractions)	Vertical thermal conductivity at 20°/100° (W/mK)
Upper North Sea Group (NU)	0–23	Deposition	50% Sand, 50% Shale	2.54/2.36
Middle North Sea Group (NM)	23–34	Deposition	60% Shale, 40% Sand	2.38/2.20
Pyrenean	34–36	Erosion	–	–
Lower North Sea Group (NL)	36–62	Deposition	75% Shale, 25% Sand	2.04/1.99
Laramide	62–68	Erosion	–	–
Ommelanden Formation (CKGR)	68–85	Deposition	75% Limestone, 25% Shale	2.58/2.38
Sub-Hercynian	85–90	Erosion	–	–
Texel Formation (CKTX)	90–98	Deposition	100% Chalk	2.9/2.62
Rijnland Group (KN)	98–141	Deposition	100% Shale	1.64/1.69
Coevorden Formation (SKCF)	141–143	Deposition	75% Shale, 25% Limestone	1.72/1.75
Weiteveen Formation (SKWF)	143–161	Deposition	75% Shale, 20% Salt, 10% Limestone	2.29/2.17
Kimmerian	161–170	Erosion	–	–
Posidonia Shale Formation (ATPO)	170–190	Deposition	100% Shale	1.25/1.41
Altena Group (AT)	190–213	Deposition	75% Shale, 25% Silt	1.73/1.76
Upper Germanic Trias Group (RN)	213–240	Deposition	75% Shale, 25% Silt	1.73/1.76
Lower Germanic Trias Group (RB)	240–245	Deposition	34% Shale, 33% Silt, 33% Sand	2.36/2.22
Zechstein Group (ZE)	245–257	Deposition	100% Salt	6.5/5.25
Upper Rotliegend Group (RO)	257–289	Deposition	80% Sand, 20% Shale	3.31/2.92
Base-Permian	270–295	Erosion	–	–
Hunze Subgroup (DCH)	304–307	Deposition	57% Sand, 42% Shale, 1% Coal	2.66/2.44
Dinkel Subgroup (DCD)	307–311.5	Deposition	62% Shale, 35% Sand, 3% Coal	2.13/2.04
Caumer Subgroup (DCC)	311.5–319	Deposition	50% Shale, 45% Sand, 5% Coal	2.24/2.13
Geul Subgroup (DCG)	319–325	Deposition	85% Shale, 15% Sand	1.82/1.82
Carboniferous Limestone Group (CL)	325–357	Deposition	75% Limestone, 25% Shale	2.11/2.04
Pre-Carboniferous sedimentary basement	357–400	Deposition	60% Shale, 40% Sand	2.38/2.20
Crystalline basement	400–415	Deposition	100% Granite	2.67/2.40

et al. (2007)). Following these heat flow peaks, asymptotically declining heat flows back to “normal” over 50 million years were applied following the reasoning of McKenzie (1978). Present-day basal heat flows were calibrated according to available temperature data from wells. The upper thermal boundary condition consists of two elements, the paleowater depth and the sediment–water-interface-temperature (SWIT). The paleowater depth was set according to TNO-GSN (2020c). The SWIT was calculated using the built-in PetroMod calculator including the paleowater depth history and the paleogeographical latitude (Wygrala 1989). For this, a present-day latitude of 52° N was set, representing the northern Netherlands.

Calibration

Twenty-eight wells, for which borehole temperature and vitrinite reflectance data are available, were calibrated as 1D models; the resulting burial, erosion and temperature histories were used to build the 3D model. By comparing the calculated temperatures and vitrinite reflectance values using the Easy %R_oDL approach from Burnham et al. (2016) to measured data, the thermal evolution and the burial history of the well locations were reconstructed. The Easy %R_oDL kinetic was used to calculate the vitrinite reflectance of buried layers and is regarded as an improvement to the Sweeney and Burnham (1990) Easy %R_o algorithm (Schenk et al. 2017; Froidl et al. 2020a). Vitrinite reflectance is calculated for all layers, no matter whether they contain organic matter or not, but calibration can only be performed for layers containing vitrinite.

Petroleum systems

Hydrocarbon generation kinetics were used to calculate the petroleum generation and transformation ratio of Cretaceous, Jurassic, and Carboniferous source rock intervals. Average thicknesses, thickness ranges, initial HI and TOC values illustrated in Table 2 were assigned to major source rock intervals (Bruns et al. 2016). A kerogen Type III kinetic from Froidl et al. (2020a) was assigned to the Caumer Subgroup (Fig. 5b; 250 mg HC/gTOC; 2% TOC), whereas the Pepper and Corvi (1995) TII kinetic was selected for the marine Posidonia Shale (550 mg HC/gTOC; 2% TOC). The

petroleum generation of the lacustrine Coevorden Formation (Fig. 5c; 700 mg HC/gTOC; 12% TOC), referred to as Wealden Shale, was calculated using a kinetic from Froidl et al. (2020b).

Results

Seismic interpretation

Thirteen marker horizons subdivide the 3D seismic-reflection data used in this study into 12 seismic units representing the key stratigraphic units in the study area (NAM and RGD 1980; Van Adrichem Boogaert and Kouwe 1994; TNO-GSN 2020c).

The lowermost and oldest seismic unit corresponds geologically to the upper part of the Limburg Group (Figs. 6, 7). This unit is characterized by low to medium amplitudes, low frequencies, and low to medium continuous reflections with locally dipping or rotated reflectors (Fig. 6a). There are areas with irregular reflection patterns mainly attributed to the poor seismic quality of this section. The units thickness ranges from 1200 to > 5000 m (Fig. 4; TNO-GSN 2020a, b). The overlying Rotliegend Group is present in the northern half of the study area but only locally in the south with a low thickness (Fig. 7a). The unit reaches a thickness of up to 500 m in the north and thins towards the south (Fig. 4; TNO-GSN 2020a). It features mostly medium amplitudes, medium frequencies, and high continuity reflections with a sub-parallel to parallel reflection pattern that is often offset by faults. In contrast, seismic reflectors of the Zechstein Group range from low to medium frequencies, low amplitudes, and overall low to medium continuities and complex reflection patterns. A set of high amplitude and high continuity reflectors is present at the base and in the upper part of the seismic unit. Figures 4, 6a and 7a show the highly variable thickness of the unit (locally up to 3700 m; TNO-GSN 2020a). The Lower Germanic Trias Group is characterized by low amplitudes, medium to low frequencies, and semi-continuous reflectors. It is lacking on large parts of the Friesland Platform as well as the Groningen Platform and locally across the study area, but can reach a thickness of 1500 m in the northeast (Figs. 4, 6a; TNO-GSN 2020a). In contrast to the underlying units, reflectors of the Upper

Table 2 Assigned source rock properties (Bruns et al. 2016) and kinetics used (Pepper and Corvi 1995; Froidl et al. 2020a, b)

Source rock	Initial hydrocarbon index (mgHC/gTOC)	Initial total organic carbon (%)	Source rock thickness (m)	Average thickness (m)	Kinetic
Coevorden Formation	700	12	0–300	12	Froidl et al. (2020b)
Posidonia Shale formation	550	2	0–390	2	Pepper and Corvi(1995)
Caumer Subgroup	250	2	100–2000	950	Froidl et al. (2020a)

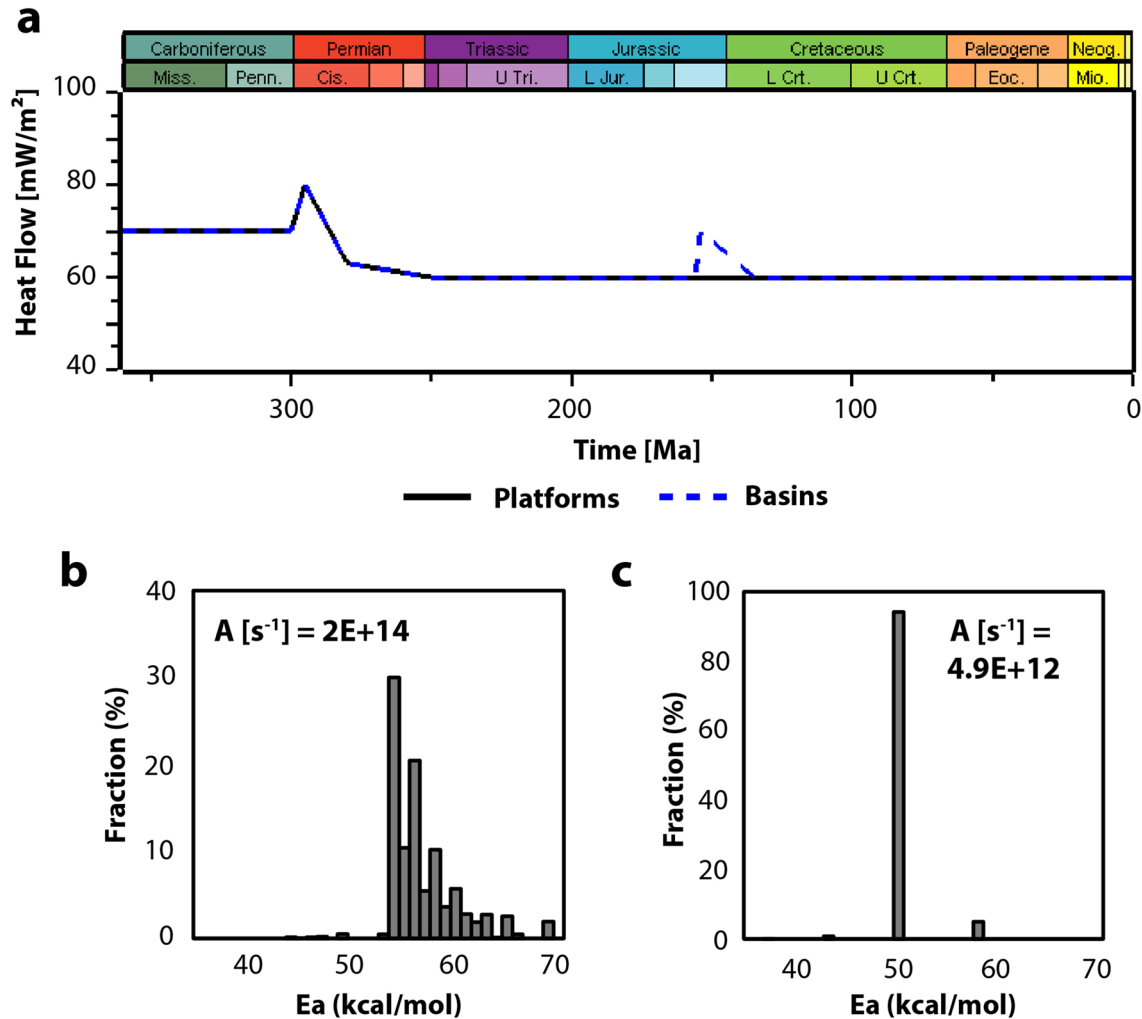


Fig. 5 **a** General modeled basal heat flows in the platforms and basins based on the McKenzie approach and according to Uffman and Littke (2011) and Bruns et al. (2016). High basal heat flows are set to periods of rifting, in the Permian and Late Jurassic. **b** Kinetic model from

Froidl et al. (2020a) assigned to the Carboniferous source rock intervals. **c** Kinetic model from Froidl et al. (2020b) assigned to the Wealden Shale/Coevorden formation

Germanic Trias Group can be identified by sets of high amplitude reflectors and generally higher amplitudes as well as higher continuity (Fig. 6a). This unit is just locally present (Fig. 7a) and it overall thickens to the east with a maximum of > 1850 m (Fig. 4; TNO-GSN 2020a). The Altena Group features mostly low amplitudes, low frequencies but continuous reflectors and is only present in the Jurassic basins with a thickness of up to 550 m (Figs. 4, 6; TNO-GSN 2020a). Figure 7a shows a set of high amplitude reflections with a high continuity that is locally present in the upper part of the Altena Group representing the Posidonia Shale formation (ATPO). Like the Altena Group, the Niedersachsen Group is only present in the basins. The reflections within this unit are characterized by low to medium amplitudes, medium frequencies, high continuities and parallel reflection patterns (Fig. 7a). They are often truncated at the top and the unit

reaches a maximum thickness of up to 1000 m (TNO-GSN 2020a) at the eastern boundary of the study area (Figs. 4, 6a). The Rijnland Group features continuous, medium to high frequency, and medium to low amplitude reflectors with a predominantly parallel reflection pattern in the upper part. In contrast to the underlying Jurassic Groups, the Rijnland Group is present across the study area (Fig. 4). It has a low overall thickness of up to 150 m but locally increases up to around 750 m (Fig. 4; TNO-GSN 2020a). Reflectors of the Chalk Group are characterized by medium amplitudes and sub-parallel to parallel reflector patterns. They are mostly continuous with medium to high frequencies and truncated at the boundary to the overlying layer (Fig. 6a). The thickness of the unit is highest in the east with up to 1450 m but it thins to the south as well as on top of elevated salt structures (Figs. 4, 7a). The Lower and Upper North Sea Group

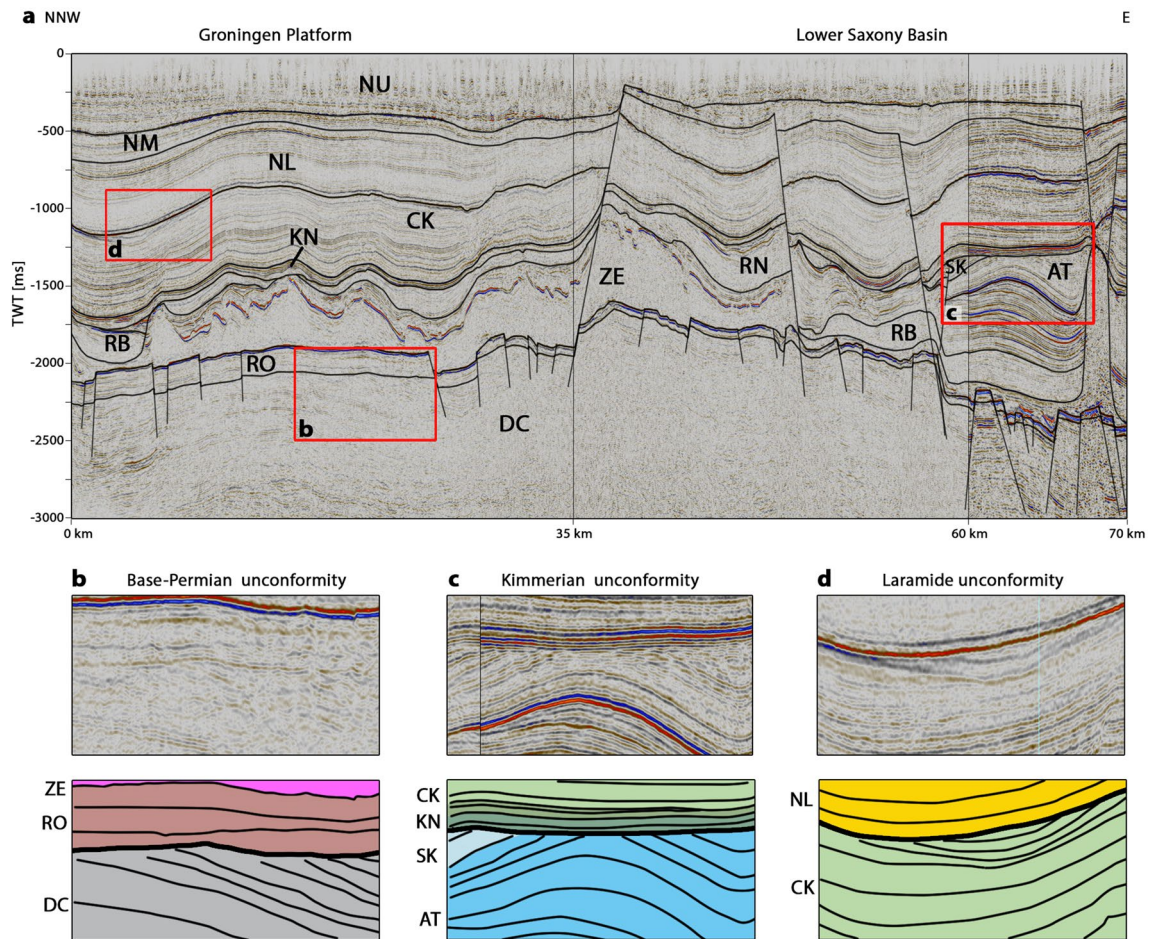


Fig. 6 **a** NNW to E directed arbitrary line 1 (for location see Fig. 1) extending from the Groningen Platform in the north to the Lower Saxony Basin in the southeast showing the highly variable thickness of the Zechstein Group as well as abundant sub-salt faults. The general stratigraphy as illustrated in Fig. 2 and differences of the struc-

tural units is shown, exemplarily the Jurassic sedimentary units that are present in the Lower Saxony Basin and absent on the Groningen Platform. Examples of identified unconformities are displayed in detail below (**b**, **c**, and **d**); colors of sedimentary units refer to colors used in the chronostratigraphic chart (Fig. 2)

feature their greatest thickness in the north and thin to the south, while the Middle North Sea Group is relatively thin across the study area. Figure 7a shows continuous reflections of the Lower to Middle North Sea Group ranging from low to high amplitudes with medium to high frequencies. In contrast, reflectors of the Upper North Sea Group show medium amplitudes and frequencies as well as medium to high continuities and in places parallel to irregular reflector patterns. Sigmoidal foresets are present in the north of the Upper North Sea Group propagating to the northeast. The thickness of the North Sea Group reaches 1750 m in the north (TNO-GSN 2020a).

Five prominent unconformities were identified based on a regional analysis of seismic-reflection terminations that were implemented into the 3D BPSM model (Figs. 6b–d, 7b, c). In the sub-salt section, the Base-Permian unconformity truncates partly rotated parallel reflections of the Limburg Group overlain by sub-horizontal parallel to sub-parallel reflections

of the Rotliegend Group (Figs. 6a, b, 7a). In areas where the Rotliegend group is missing, reflections of the Limburg Group are truncated along the Base-Permian unconformity by reflectors of the Zechstein Group (Fig. 7a). The second distinct unconformity, the Late Kimmerian unconformity, characterizes the base of the Rijnland Group, with dipping seismic-reflections overlain by relatively horizontal reflections (Figs. 6a, c, 7a). Within the Lower Saxony Basin, where sediments of the Niedersachsen and Altena Group are present, more unconformities related to the Kimmerian tectonic phase can be observed down from the Altena Group to the Upper Germanic Trias Group. The Altena Group is completely absent outside the Jurassic basins, and succeeding reflectors of the Rijnland Group unconformably overlie reflectors in places down to the Zechstein Group (Figs. 6a, 7a). Reflector truncations in the lower part of the Chalk Group relate to the Sub-Hercynian tectonic phase (Fig. 7b). In contrast to the distinct Kimmerian and Base-Permian

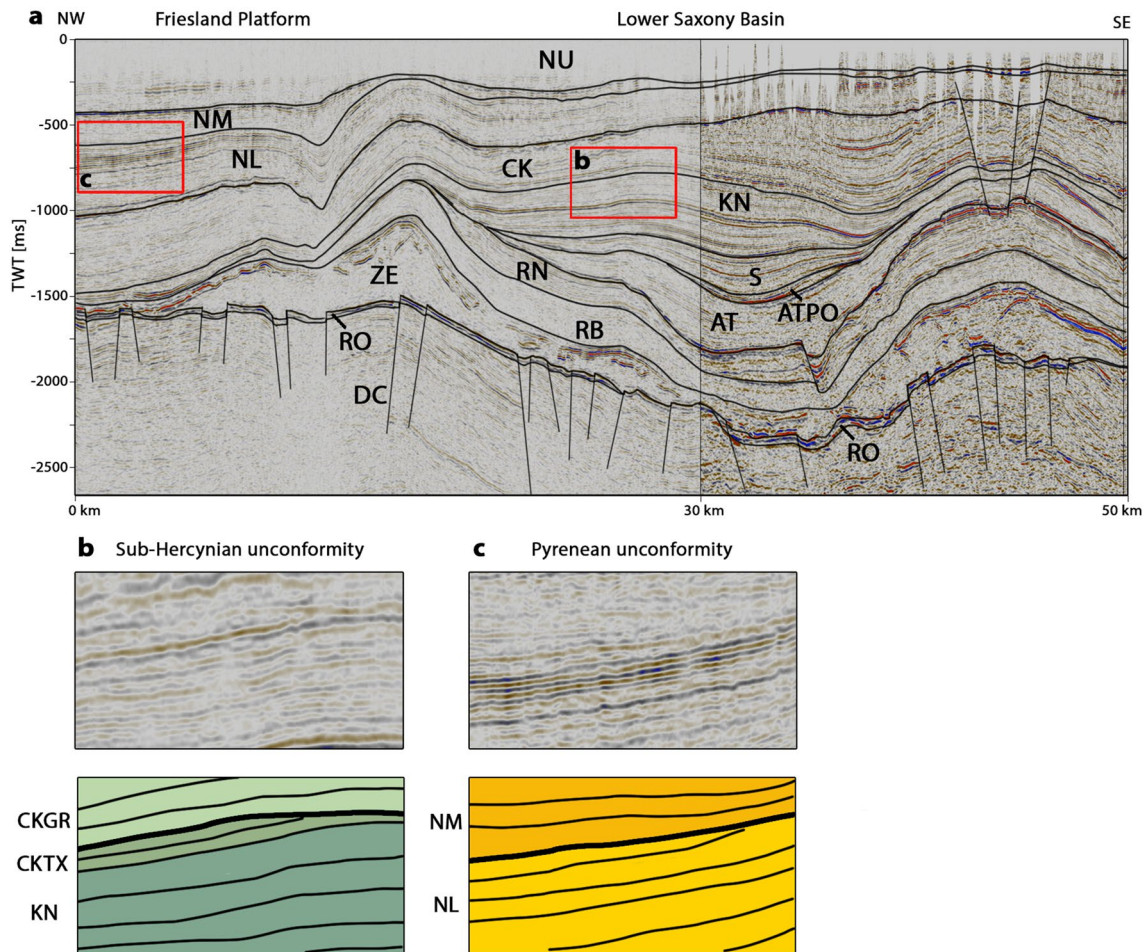


Fig. 7 a NW to SE directed arbitrary line 2 (for location see Fig. 1) extending from the Friesland Platform in the west to the Lower Saxony Basin in the east depicting the general stratigraphy as illustrated in Fig. 2 and the presence of faults in the study area. Unconformities

are present throughout the stratigraphic column. Examples of identified unconformities are displayed in detail below (b, c); colors of sedimentary units refer to colors used in the chronostratigraphic chart (Fig. 2)

unconformities, the Sub-Hercynian unconformity is in the study area characterized by truncations of only low-angle dipping reflector packages and in places difficult to observe (Figs. 6a, 7a); however, this unconformity is more prominent in the other areas such as the West and Central Netherlands Basin as a correlative conformity (Nelskamp 2011). The basinwide Laramide unconformity separates the dominantly horizontal reflections of the North Sea Group from partly inclined reflectors of the Chalk Group (Fig. 7a). This bounding surface is in most places characterized by a strong impedance contrast due to lithological changes from the carbonate dominated Chalk Group to the siliciclastic North Sea Groups and in some locations by truncations of dipping reflectors of the uppermost Chalk Group (Fig. 6d). In the uppermost North Sea Group, a couple of localized reflection truncations are present, predominantly at the boundaries of the seismic units (Figs. 6a, 7a). The most prominent of these is located at the base of the Middle North Sea Group,

identified as the Pyrenean erosional event (Figs. 6a, 7a, c). In places, an underlying package of low-angle dipping parallel reflectors with high amplitudes are truncated (Fig. 7c).

Basin modeling

The identification of major unconformities on seismic-reflection data (Figs. 6, 7) and calibration of 28 wells (Fig. 3) resulted in 5 erosional thickness maps that were implemented into the 3D BPSM model (Fig. 8). Wells on the Groningen and Friesland Platform show two major phases of erosion followed by periods of strong subsidence (Figs. 9a, b). Major erosion is observed during the Permian and during the Late Jurassic times. Late Cretaceous, Paleogene, and Oligocene erosions contribute little to the overall amount of erosion. Paleozoic sediments on most of the Groningen and Friesland platforms experienced maximum burial before Jurassic erosion. In the northern part of the platforms, the

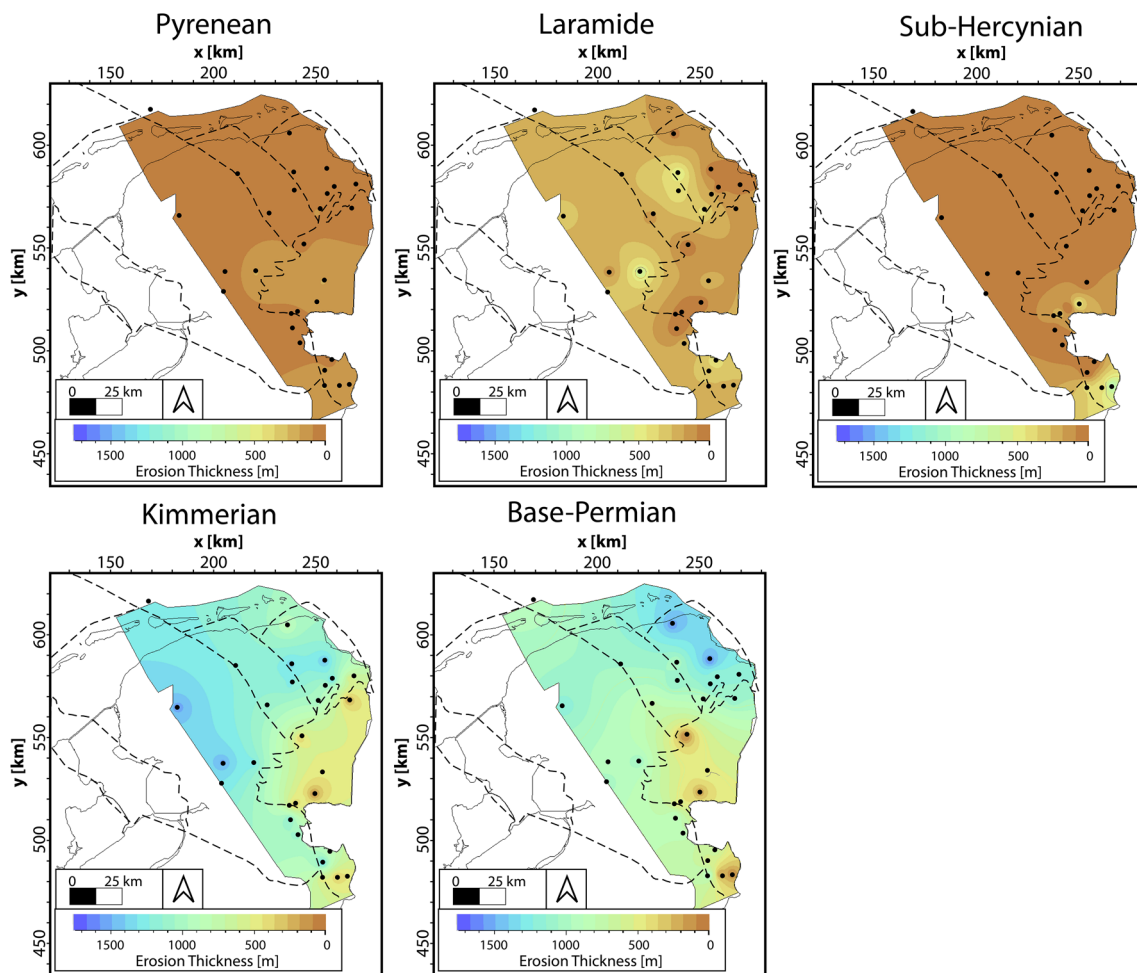


Fig. 8 Amount of erosion in five erosion events including the Pyrenean (36–34 Ma), Laramide (66–62 Ma), Sub-Hercynian (89–85 Ma), Kimmerian (170–150 Ma) and Base-Permian (290–270 Ma). Maps are based on calibrated 1D simulations on well locations and

extrapolated to the study area. Boundaries of structural elements and location of wells is indicated as dotted lines and dots (see Figs. 1 and 3)

maximum burial of Paleozoic rocks is at present-day due to still ongoing strong sedimentation initiated in Late Cretaceous times. The Lauwerszee Trough (see Fig. 1) has a quite similar burial history compared to the surrounding platforms from Mesozoic times on, but the present-day burial of Paleozoic sediments is deeper. Compared to the platforms, the basins in the study area were just mildly inverted during the Kimmerian tectonic phase, and Jurassic sediments were partly preserved (Fig. 9c, d). The amount of Base-Permian erosion of Carboniferous sediments during the Permian decreases to the southeast and is overall lower than on the platforms in the north. Because of limited Jurassic erosion, the deepest burial of Paleozoic sediments in the Dutch Lower Saxony Basin is at the present-day. In contrast, the Lower Saxony basin in the most southeastern part of the study area is characterized by a comparatively thin Cenozoic succession (Fig. 9c). There, the Carboniferous succession

experienced the deepest burial in the Cretaceous related to Sub-Hercynian erosion.

Figure 10a, b shows a fit of the modeled present-day temperatures with the available temperature data of wells in the study area. Modeled present-day temperatures at the top Carboniferous, representing the top of the major source rock interval in the study area, are highest in the north of the Lauwerszee Trough and the east of the Lower Saxony Basin (Fig. 9) with temperatures of up to 160 °C, respectively. Minimum present-day temperatures of approximately 55 °C are modeled in the south of the study area, where the top Carboniferous is buried to a depth of 1200 m at present-day. Paleozoic sediments on the platforms, in the Lower Saxony Basin, and the Lauwerszee Trough experienced maximum temperatures in the Jurassic before Kimmerian erosion and in some locations at the present-day. In the southern part of the study area, maximum temperatures were either reached during Permian or Jurassic times due to elevated heat flows

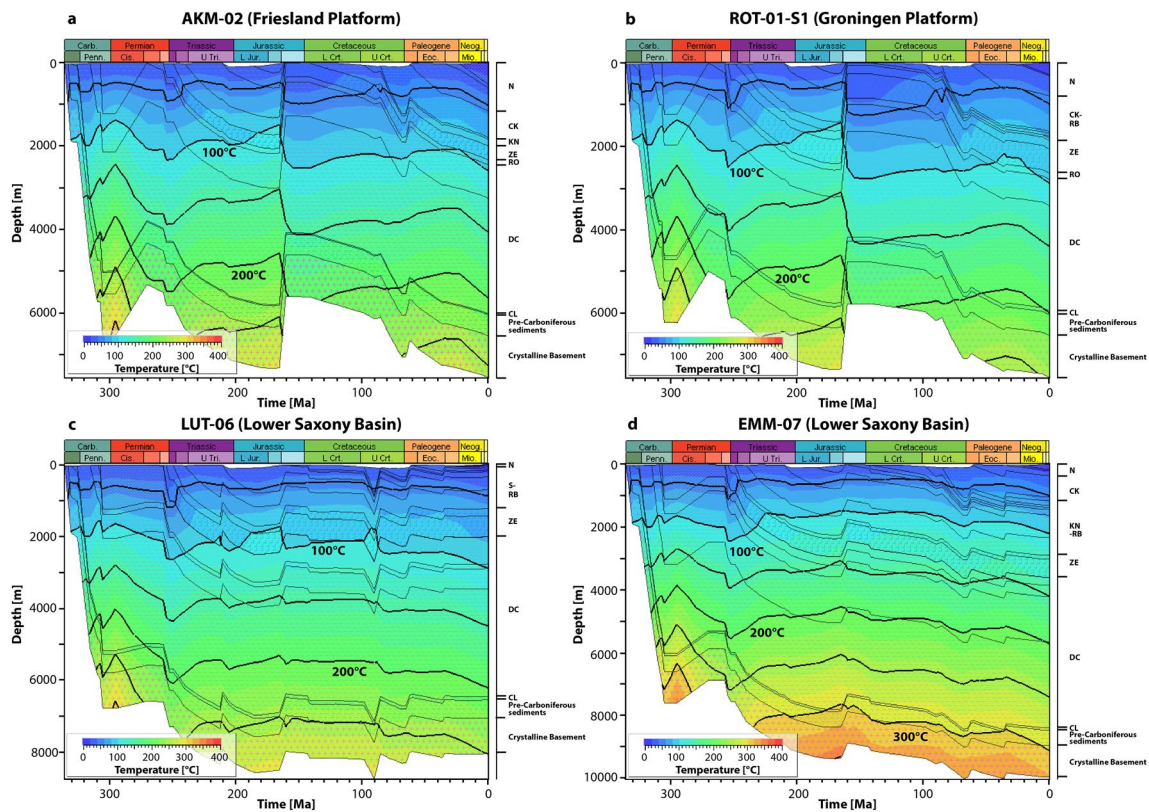


Fig. 9 Burial history with temperature overlay and 50 °C, 100 °C, 150 °C, 200 °C, 250 °C, and 300 °C isotherms of 1D extractions near the wells AKM-02 on the Friesland Platform (a), ROT-01-S1 on the

Groningen Platform (b), and LUT-06 and EMM-07 in the Lower Saxony Basin (c, d). Wells are marked in Fig. 3

and simultaneously deep burial (Fig. 9). The Mesozoic succession experienced the highest temperatures in the Late Eocene and in some areas before the Laramide erosion in the Paleogene (Fig. 9). Maximum modeled present-day temperatures of the Jurassic Altona Group (AT) and the Cretaceous Niedersachsen Group (SK) of around 95 °C are calculated in troughs between salt walls and diapirs in the Lower Saxony Basin. Present-day surface heat flows are elevated in the vicinity of salt walls and domes due to their high thermal conductivity; this mainly occurs in the east and north of the study area.

Wells with available vitrinite reflectance data were calibrated to assess the effect of subsidence, inversion, and paleo-heat flow on the stratigraphic succession across the study area. Modeled present-day maturities at the well locations fit to the vitrinite reflectance data (Fig. 10c-i). In the north, for example in the vicinity of the well USQ-01, the maturity of Paleozoic sediments slightly started to increase again in the Cenozoic due to strong sedimentation from Cretaceous times (Fig. 11). In contrast, most other wells in the Lauwerszee Trough and on the platforms show the latest increase in maturity before Kimmerian uplift (Fig. 11). In most parts of the Lower Saxony Basin, the increase in

maturity ceased during Jurassic erosion but continued from Late Cretaceous times to the present day (Fig. 11). Figure 12 shows highest present-day maturities at the top of the Carboniferous in the Dutch Lower Saxony Basin and the Lauwerszee Trough with modeled maturities up to 3.5 % R_o . Westphalian sediments with lowest maturities down to 0.6 % R_o are calculated on the Friesland Platform and in the southernmost part of the study area (Fig. 12). On the Groningen Platform and the Lauwerszee Trough, the petroleum generation of Westphalian coals peaked during the Jurassic, was halted during the Kimmerian inversion, and resumed in areas with sufficient sedimentation and subsidence from Late Cretaceous times. Due to the deeper burial of Paleozoic sediments, petroleum generation in the Lauwerszee Trough is more advanced in comparison to the surrounding platforms as shown in Fig. 13. The hydrocarbon generation history of Westphalian coals on the Friesland Platform is similar, but present-day transformation ratios are lower. In basins that did not experience such a severe uplift in Jurassic times compared to the platforms, hydrocarbon generation continued during the Jurassic to Cretaceous times due to subsequent subsidence. Throughout the study area, the highest present-day transformation ratios are observed in

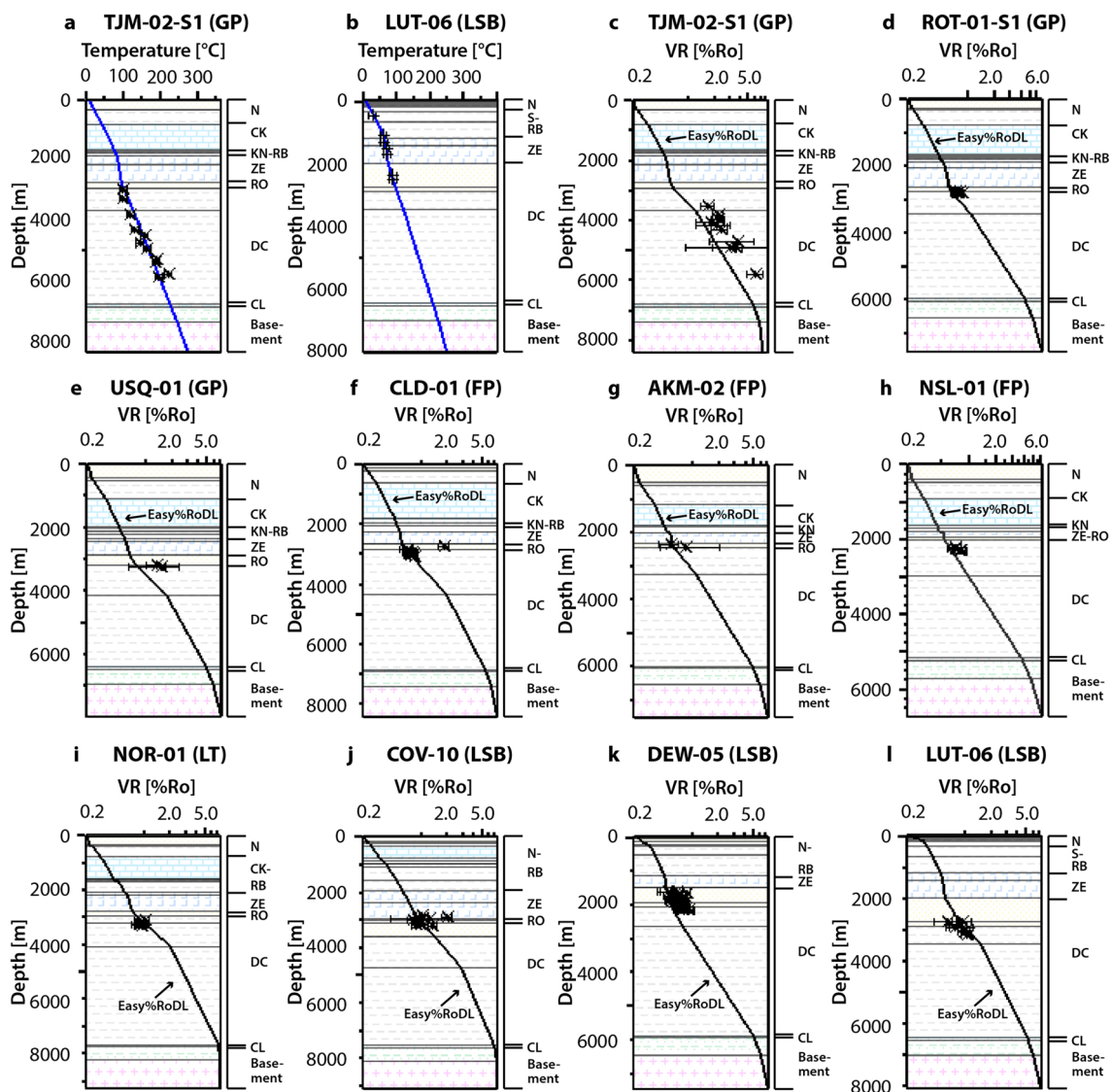


Fig. 10 Calculated present-day temperatures with corrected temperature measurements (a, b) and present-day maturity calibrations using Easy %R_oDL with vitrinite reflectance data (c–l) of 1D extractions near selected wells on the Groningen Platform (TJM-02-S1, ROT-01-S1, USQ-01), the Friesland Platform (CLD-01, AKM-02, NSL-

01), the Lauwerszee Trough (NOR-01) and in the basins (COV-10, DEW-05, LUT-06) as shown in Fig. 3. Dots and crosses show available temperature and vitrinite calibration data with assigned error margins of 10 °C for corrected temperature data from Bonte et al. (2012) and min/max margins for vitrinite reflectance measurements

areas with limited Base-Permian and Kimmerian erosion in the east (Fig. 13) and the partial presence of Stephanian and Jurassic sediments.

Jurassic and Cretaceous source rocks are only preserved in the basins and have low overall calculated present-day maturities. The Posidonia Shale, only locally present, has highest modeled present-day maturities of 0.55 %R_o and only shows negligible transformation ratios of up to 1% (Fig. 14a). Highest temperature is observed during Paleogene times, while the strongest increase in maturity of the Posidonia Shale is calculated from the Cretaceous to the Paleogene. In contrast to the Posidonia Shale that

is preserved in most parts of the Dutch LSB, the Wealden Shale is in parts early oil mature with modeled maturities of up to 0.57 %R_o in troughs between salt walls and domes. Petroleum generation of the Wealden Shale is limited to such troughs, in which transformation ratios of up to 7.5% are calculated (Fig. 14b). A strong maturity increase and the start of the petroleum generation is calculated in the Late Cretaceous related to strong sedimentation and subsequent subsidence. The highest temperature was reached prior to Pyrenean erosion during the Eocene.

Fig. 11 Maturity (Easy %R₀DL) and temperature evolution at the top of the Limburg Group (DC), comprising the main source rock intervals, on different structural elements. Well NSL-01 is located on the Friesland Platform and well USQ-01 on the Groningen Platform showing the general trend on platforms, well NOR-01 is situated in the Lauwerszee Trough and well GRL-01 in the Lower Saxony Basin. The exact amount of calculated vitrinite reflectance differs across the structural elements

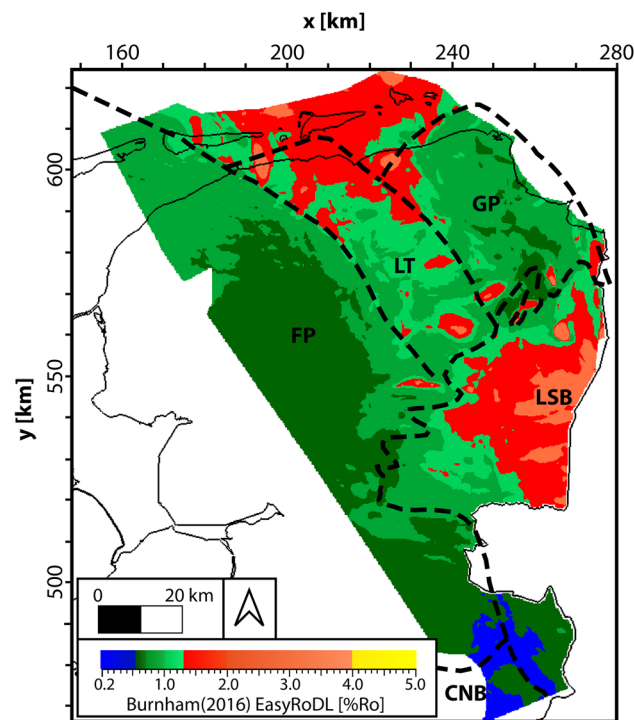
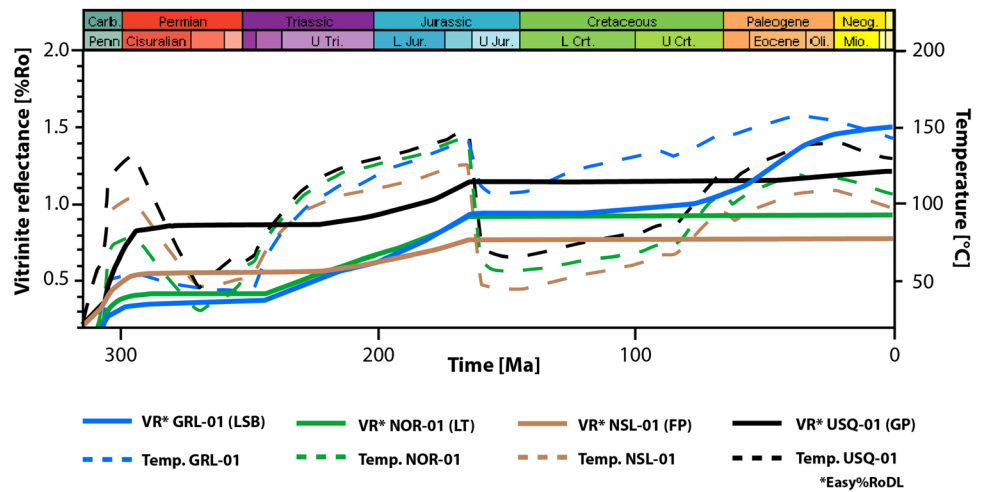


Fig. 12 Calculated present-day maturity map at the top of the Carboniferous succession using Easy %R₀DL. Main structures are outlined with black solid lines

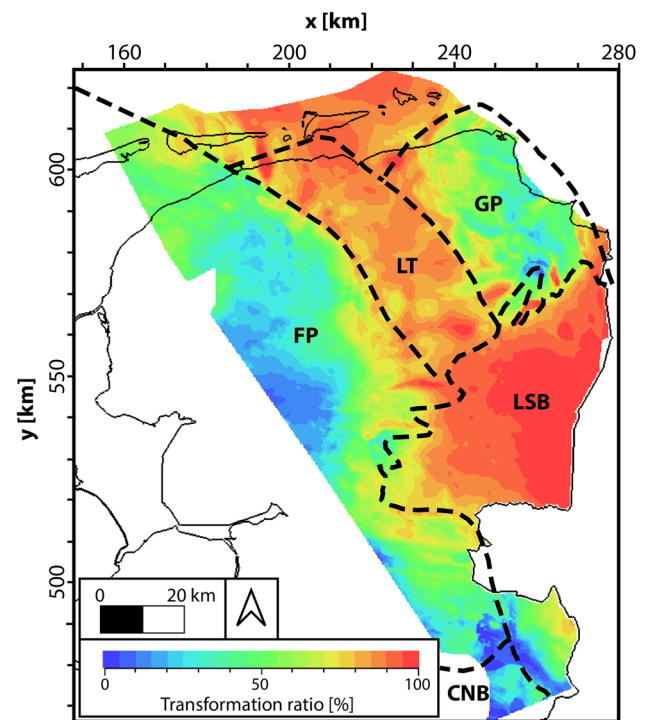


Fig. 13 Calculated present-day transformation ratio map at the top of the Caumer Subgroup comprising the major Westphalian coal succession using a kinetic from Froidl et al. (2020a). Main structures are outlined with black solid lines

Discussion

Four important assumptions have been made which reflect the uncertainty in the large-scale basin model, presented:

First, the structural element Dalfsen High, located in the southwest of the study area (Fig. 1), is treated as a platform like the surrounding Friesland Platform for the temperature and maturity history modeling. However, it should be noted that there are no vitrinite reflectance data in this rather small area (Kombrink et al. 2012).

Second, the Carboniferous succession was subdivided using well picks from 14 wells that penetrated parts of the Carboniferous succession across the study area. The Caumer Subgroup comprises the Maurits, Ruurlo and Baarlo formations, deposited in the Westphalian A to Early Westphalian C, with coal seams therein forming the most important source rock. The thickness of the Caumer Subgroup ranges from 1000 to 2000 m in the Lower Saxony Basin, the

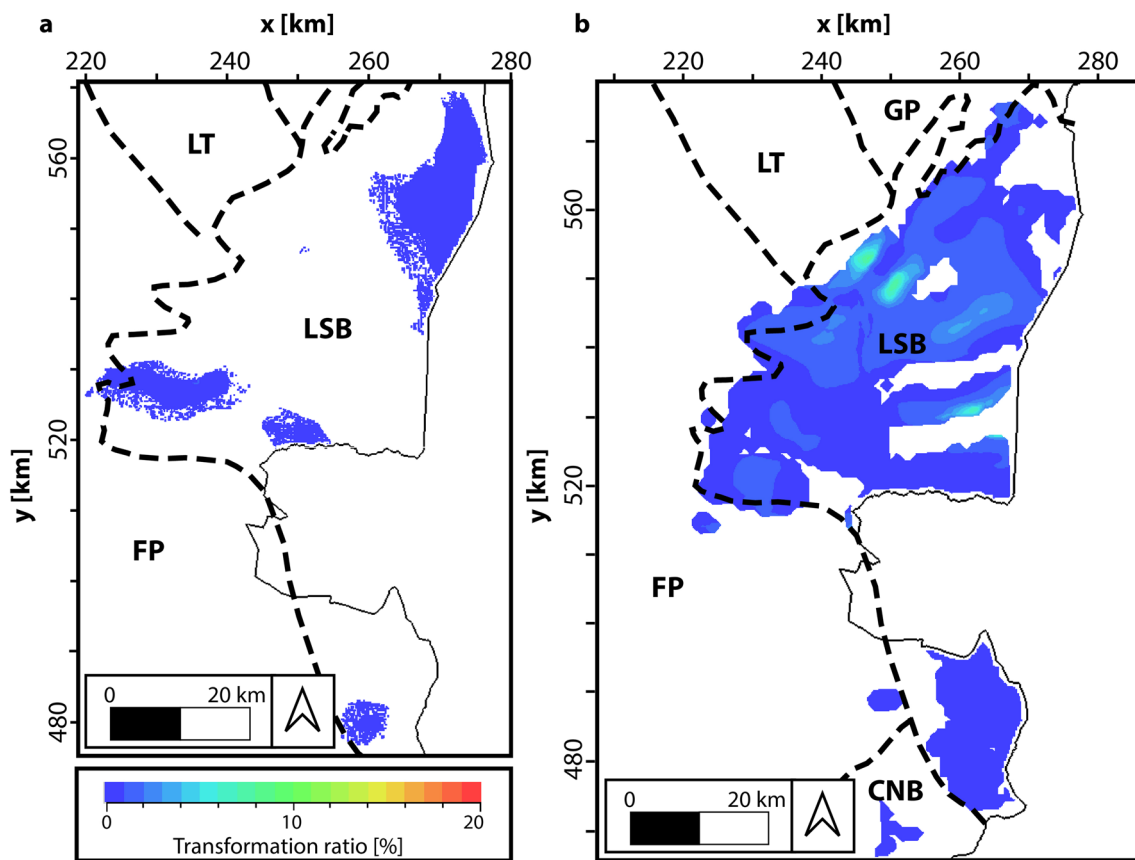


Fig. 14 **a** Calculated present-day transformation ratio maps at the top of the Posidonia Shale using a kinetic from Pepper and Corvi (1995). **b** Calculated present-day transformation ratio maps at the top of the Wealden Shale using a kinetics from Froidl et al. (2020b). A maxi-

mum of 20% transformation ratio is displayed due to general low values as indicated in the color bar. Main structures are outlined with black solid lines

western Friesland Platform and Lauwerszee Trough. In the Groningen Platform, the northern Friesland Platform, and the southernmost part of the study area, most of the unit is between 500 and 1000 m thick. However, most of the wells do not penetrate the lower boundary of the Maurits formation. Therefore, the Caumer Subgroup was not further subdivided based on well picks, but a mixed lithology (Table 1) was used to account for the low thermal conductivity of coal in the alternating successions of siliciclastic sediments and coal seams in varying amounts. Additionally, seismic-reflection data of the Limburg Group shows relatively low impedance contrasts in between siliciclastic sediments and a high impedance contrast of coal seams (Figs. 6, 7; van Buggenum and den Hartog Jager 2007). Because coal seams differ in their thickness, vary in their regional presence and are difficult to trace across a large area, the entire Caumer Subgroup was assigned as a source rock interval (Table 2).

Third, the Zechstein Group was implemented as one homogenous layer of salt, although it comprises several evaporitic cycles and sequences (Warren 2008; Strozyk et al. 2017). This is shown by the complex structure of the

Zechstein unit in the seismic-reflection sections (Figs. 6, 7). In reality, most of the tectonic deformation was accommodated by the Z2 salt unit, whose primary thickness is estimated to reach 500 m (Strozyk et al. 2017). As the in-built facies piercing tool has been applied to estimate the vertical movement of salt in this large-scale 3D model, no lateral salt movement is considered. This potentially affects the source rock maturation near elevated salt successions.

Finally, the paleo heat flow scenarios based on the classical approach from McKenzie (1978) are used in large-scale models of the CEBS such as Adriasola Munoz et al. (2007), Uffmann and Littke (2011), Bruns et al. (2013) and Bruns et al. (2016). In these, a Permian heat flow peak occurs throughout the study area, while the area of the Lower Saxony Basin is characterized by a second heat flow peak related to rifting in the Jurassic. This heat flow approach was used and adapted to calibrate 1D simulations at 28 well locations. Final heat flows of these simulations were extrapolated and used as the lower thermal boundary for the 3D model through time. To validate the calibration results obtained from 1D modeling in the 3D model, 1D extractions

at all well locations were done (Fig. 10). The results are in accordance with the initial 1D calibration results, despite the additional effects of heat transport in 3D and temperature disturbances caused by salt diapirs (Magri et al. 2008). Van Wees et al. (2000, 2009) published an alternative approach taking the tectonic subsidence, sedimentation rates, and other factors into account. Paleo heat flow maps from this approach were used as an additional scenario in a model by Bruns et al. (2016), covering the extent of the 3D model in this study. Comparing both approaches in this study area, the paleo heat flow is higher in the McKenzie approach and elevated, particularly during phases of crustal thinning. Heat flow maps of the probabilistic scenario of the 3D model of Bruns et al. (2016) were used but do not significantly change the modeling results concerning the maturity and transformation ratio of source rocks.

The overall subsidence history of the platforms and the Lauwerszee Trough is similar to other adjacent platforms such as the Cleaverbank Platform (Abdul Fattah et al. 2012). The modeled geological evolution of the Dutch Lower Saxony Basin is in line with the results of other basin modeling studies in salt-dominated and inverted Jurassic basins in the Netherlands (Verweij 2003; Nelskamp 2011; Verweij et al. 2012; Bouroulllec et al. 2019; Bonte et al. 2020). Erosion in the Jurassic related to the Kimmerian tectonic phase is simulated in this study and other studies by Groetsch et al. (2011) and Abdul Fattah et al. (2012) as one strong event that predominantly affected the platforms in places down to the Permian (to a much lesser extent the Lower Saxony Basin). This unconformity occurs at the base of the Lower Cretaceous Rijnland Group (Fig. 6c) and is related to the culmination of the disintegration of the Southern Permian Basin into several sub-basins starting in the Triassic (Geluk 2007). Other erosional intervals associated with tectonic phases (Lower Triassic Hardegsen) can be observed as unconformities on seismic data in various other parts of the study area (Figs. 6a, 7a). As a result of the erosion triggered by the Pyrenean collision event in the Eocene, only a thin cover of Paleogene and Neogene sediments are preserved in the most southern part of the study area at the boundary of the Lower Saxony Basin to the Central Netherlands Basin (De Jager 2003). In this area, strong erosion took place in the Campanian Sub-Hercynian and Paleocene Laramide phases, as illustrated in erosion maps derived from 1D calibrations (Figs. 8, 9c).

Observations regarding the present-day heat distribution in the subsurface are in accordance with published data from Uffmann and Littke (2011), Scheck-Wenderoth and Maystrenko (2013), Bruns et al. (2016), and Bekesi et al. (2020). Variations in present-day temperatures related to salt domes creating a chimney effect due to locally high thermal conductivities are present across the study area (Magri et al. 2008). A sensitivity analysis was carried out to investigate

the effects of changes in the heat flow and different extent of erosions during two decisive phases of burial and subsequent erosion in the Late Carboniferous and Jurassic (Fig. 15). Figure 15a shows the variation of the heat flow in 10 mW/m² steps from the best fit scenario. The best fit scenario assumes high heat flows at times of extensional tectonics (Fig. 5) as used in previous studies by Uffmann and Littke (2011) and Bruns et al. (2016). Well ROT-01-S1 is located on the Groningen Platform (Fig. 3), where heat flows were enhanced during Late Carboniferous to Early Permian times (Fig. 5a). To illustrate the effect of changes in paleo heat flows, different heat flows during the Early Permian, the Late Jurassic and from Paleogene to Neogene times are tested. Scenarios were applied incrementally increasing heat flows by 10 mW/m² for the Early Permian, Late Jurassic and Paleogene to Neogene. By increasing the basal heat flow to 80 mW/m² or higher during maximum burial in Late Jurassic times (Fig. 15a; blue lines), calculated maturities are too high compared to measured data. Increasing the heat flow values during the Early Permian does not show a significant change of the calculated maturity, but rather changes the gradient of the maturity curve in the Limburg and Carboniferous Limestone Groups (Fig. 15a). Increasing the paleo heat flow during the Paleogene to Neogene has a strong influence on the overall maturity (Fig. 15a) of well ROT-01-S1 due to strong sedimentation from Late Cretaceous times on (Fig. 9b). Second, the influence of the eroded sediment thickness was assessed (Fig. 15b). This was done increasing the thickness of eroded sediment by 500–2000 m during two phases of burial and erosion in the Late Carboniferous to Early Permian and Jurassic (Fig. 8). Indicated by the presence of basinwide unconformities on seismic data, both times are thought to be decisive phases in the geological evolution of the area (Fig. 6b, c). In the best fit model of well ROT-01-S1 (Fig. 15), an eroded sediment thickness of 1150 m assigned to the Base-Permian erosion and 1300 m of eroded sediments related to the Kimmerian erosion were set (Fig. 8). Eroded sediment thicknesses of above 1600 m for the Early Permian erosion and above 1500 m for the Jurassic phase yield calculated maturities that are too high for well ROT-01-S1 using the heat flow scenario described above. Vitrinite reflectance measurements across a higher number of sedimentary formations in more depth intervals could help to further delimit possible heat flow and erosion scenarios. High erosion thicknesses of Carboniferous sediments are found in other modeling studies such as Schroot et al. (2006) and are indicated by locally preserved Carboniferous sediment thicknesses of above 5500 m (Fig. 4; Van Buggenum and den Hartog Jager 2007). The thickness maps of Mesozoic units (Fig. 4) show the partial absence of the Niedersachsen, Altena, and Germanic Trias Group and the effect of strong erosion during the Mesozoic. The influence of both burial phases on the maturity of the Paleozoic source

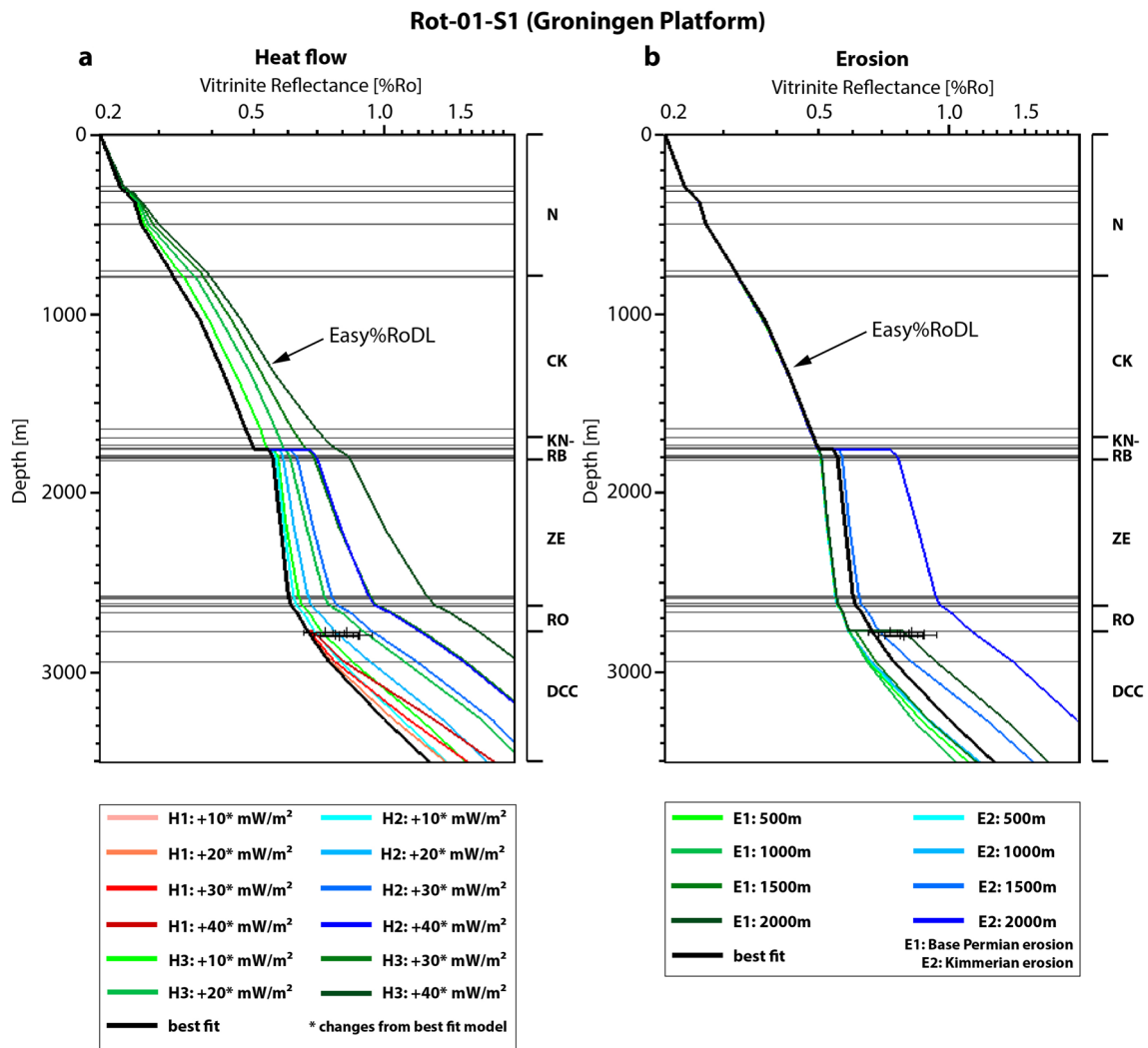


Fig. 15 Sensitivity analysis for the well ROT-01-S1 located on the Groningen Platform. Available vitrinite reflectance measurements are located in the upper part of the Carboniferous Limburg Group. Crosses show available vitrinite calibration data with min/max margins for vitrinite reflectance measurements. **a** Variations in the heat flow (Fig. 5a) in the Early Permian (H1), Late Jurassic (H2) and Cenozoic (H3) from the best fit scenario (black line) in + 10 mW/m²

steps (blue, green and red lines) and their influence on the maturity of the well. The best fit heat flow is illustrated in Fig. 5a (platforms). **b** Variations in the amount of Base-Permian (E1) and Kimmerian (E2) erosion and burial (black line; amount of erosion in Fig. 8) in ± 500 m steps (blue and green lines) and their influence on the maturity of the well

rocks is also stated in other studies on the area (Groetsch et al. 2011; Nelskamp 2011). Eroded sediment thicknesses during the Sub-Hercynian, Laramide, and Pyrenean phases do in most places not exceed a maximum of a couple of hundred meters of eroded sediments. Thus, erosion events during the Paleogene and Neogene did not contribute significantly to the overall maturity of the succession.

The strongest increase in the maturity and transformation ratio of Westphalian source rocks is observed before the area experienced severe uplift and erosion related to the Kimmerian phase (Fig. 11). The maturity did not further increase in most of the platform areas but resumed in the north due to strong sedimentation (Groetsch et al. 2011). Because of

limited Kimmerian erosion and subsequent deeper burial in the Lower Saxony Basin, maturities are higher than in platform areas. An accelerated hydrocarbon generation in the Jurassic rift basins was described by De Jager and Geluk (2007) during Late Jurassic to Early Cretaceous times. For the Lower Saxony Basin, this is not in agreement with the results presented, as there is no increase in the overall maturity due to limited erosion in the Late Jurassic (Figs. 9d, 11). In other Dutch rift basins such as the West Netherlands Basin, an increased generation of hydrocarbons during the Jurassic was modeled by van Balen et al. (2000) and Nelskamp (2011). Other observed trends are in line with published data from Uffmann and Littke (2011), but the results

of this study show a more detailed maturity distribution across the northeastern onshore part of the Netherlands.

Mesozoic source rocks such as the Posidonia Shale and Wealden Shale are only sparsely present in the study area and have relatively low modeled maturities. Maturities of the Posidonia shale are in accordance with published measured and modeled maturity data of adjacent areas in the Western Netherlands Basin and the Lower Saxony Basin in Germany (Song et al. 2015; Bruns et al. 2016). In comparison to the central part of the Lower Saxony Basin, in which maturities of up to 4 % R_0 were reached before strong Late Cretaceous inversion, the Posidonia Shale is immature to early oil mature in the study area and did not significantly contribute to hydrocarbon accumulations (Fig. 14a) in the Dutch Lower Saxony Basin whereas it likely did in other parts of the CEBS (Maystrenko et al. 2008; Bruns et al. 2016; Stock and Littke 2018).

The large Schoonebeek oil field at the Dutch border to Germany is thought to be sourced by the Wealden Shale of Berriasian age and not by the Posidonia Shale (Wehner et al. 1989; De Jager and Geluk 2007). Geochemical data indicate that the oil was expelled from the Wealden Shale during the “early oil window” stage at maturities of up to 0.7 % R_0 (Wehner et al. 1989). In published kinetic data by Ziegls et al. (2015), temperatures of 160 to 170 °C, with a heating rate of 3 °C/Ma, are needed for peak petroleum generation from the Wealden, which is not consistent with oil and source rock maturities in the area (Wehner et al. 1989; Bruns et al. 2016). A new, improved kinetic data set for the Wealden Shale by Froidl et al. (2020b) was used in this study, in which peak petroleum generation is starting at around 130 °C. According to modeled maturities, the Wealden Shale is in places in the early oil window and started to produce hydrocarbons with maximum transformation ratios ranging from 5 to 8% (Fig. 14b). Migration of these early generated hydrocarbons to suitable reservoirs is, therefore, possible. Published data from Bruns et al. (2016) and Froidl et al. (2020b) indicate higher maturities of the Wealden Shale to the east in the central part of the Lower Saxony Basin, in which the source rock experienced higher temperatures due to deeper burial.

Conclusion

The most recent subsurface model of the Netherlands (DGM-deep v5) and additional published data were used to reconstruct the burial and temperature history of the sedimentary succession from Carboniferous to recent times in onshore northeastern Netherlands in a large-scale petroleum systems 3D model. Seismic interpretation was used to identify five unconformities related to major erosion events that were implemented in the 3D basin and petroleum system model. 3D modeling reveals strong variations in the

present-day temperature and the thermal maturity maps of Carboniferous source rocks depending on the location within one of the structural elements. Maturities of Paleozoic source rocks are lowest on the Friesland Platform in the west and the most southern area and are highest in the Lauwerszee Trough and Lower Saxony Basin. Present-day temperatures show a similar trend, predominantly depending on the burial depth. Two major phases of burial and subsequent uplift influencing the thermal maturation of Paleozoic sediments are observed. The first deep burial and maturation occurred during Carboniferous prior to Base-Permian erosion and a second phase from Triassic to Jurassic times before Kimmerian erosion. During subsequent burial from the Late Cretaceous times onwards, hydrocarbon generation resumed in the northern part of the study area.

Mesozoic source rock intervals are mainly limited to the Dutch Lower Saxony Basin. The Toarcian Posidonia Shale is just present in a few locations within the Lower Saxony Basin, while the Berriasian Wealden Shale is present across a larger area in the Lower Saxony Basin and two locations within the Groningen platform. An increase in maturity of both source rocks is mainly driven by burial from Cretaceous to Paleogene times for the Posidonia Shale and from Cretaceous to Eocene times for the Wealden Shale. The 3D basin and petroleum systems model shows that both source rock intervals are in parts early oil mature, for example, in trenches between salt diapirs. Transformation ratios of the kerogen type II Posidonia Shale are very low. In contrast, the Wealden Shale containing kerogen type I started to generate hydrocarbons indicating a potential source for nearby oil fields in the Dutch LSB. Utilizing 3D basin modeling and depth maps with a high spatial resolution, the provenance of oil in hydrocarbon fields of the western LSB can thus be possibly further resolved using recently published kinetic data.

Acknowledgements This study was funded by the Deutsche Forschungsgemeinschaft (DFG, German Research Foundation), Project SA 3094/4-1. We thank TNO for providing the 3D seismic-reflection data and the public databases NLOG (<http://www.nlog.nl>) and DINOLoket database (<http://www.dinoloket.nl>). Finally, we thank reviewer Susanne Nelskamp and an anonymous reviewer for their constructive comments, which helped to improve the manuscript.

Funding Open Access funding enabled and organized by Projekt DEAL. This study was funded by the Deutsche Forschungsgemeinschaft (DFG, German Research Foundation)—SA 3094/4-1.

Availability of data and materials Input data (e.g. depth maps, well data, vitrinite reflectance measurements, borehole temperatures) used in this study is publicly available in TNO’s NLOG and DINOLoket databases.

Code availability Not applicable.

Declarations

Conflict of interest The authors declare that they have no known competing financial interests or personal relationships that could have appeared to influence the work reported in this paper.

Open Access This article is licensed under a Creative Commons Attribution 4.0 International License, which permits use, sharing, adaptation, distribution and reproduction in any medium or format, as long as you give appropriate credit to the original author(s) and the source, provide a link to the Creative Commons licence, and indicate if changes were made. The images or other third party material in this article are included in the article's Creative Commons licence, unless indicated otherwise in a credit line to the material. If material is not included in the article's Creative Commons licence and your intended use is not permitted by statutory regulation or exceeds the permitted use, you will need to obtain permission directly from the copyright holder. To view a copy of this licence, visit <http://creativecommons.org/licenses/by/4.0/>.

References

- Abdul Fattah RA, Verweij JM, Witmans N, Ten Veen JH (2012) Reconstruction of burial history, temperature, source rock maturity and hydrocarbon generation in the northwestern Dutch offshore. *Neth J Geosci* 91(4):535–554. <https://doi.org/10.1017/S001677460000378>
- Adriasola Munoz Y, Littke R, Brix MR (2007) Fluid systems and basin evolution of the western Lower Saxony Basin, Germany. *Geofluids* 7(3):335–355. <https://doi.org/10.1111/j.1468-8123.2007.00186.x>
- Allen PA, Allen JR (2013) Basin analysis: principles and application to petroleum play assessment. Wiley, New York (ISBN: 978-0-470-67377-5)
- Bachmann GH, Voigt T, Bayer U, von Eynatten H, Legler B, Littke R (2008) Upper Rotliegend to early cretaceous basin development. In: Littke R, Bayer U, Gajewski D, Nelskamp S (eds) Dynamics of complex intracontinental basins. Springer, Berlin, pp 152–172. https://doi.org/10.1007/978-3-540-85085-4_4
- Békési E, Struijk M, Bonté D, Veldkamp H, Limberger J, Fokker PA, Vrijlandt M, van Wees JD (2020) An updated geothermal model of the Dutch subsurface based on inversion of temperature data. *Geothermics* 88:101880. <https://doi.org/10.1016/j.geothermics.2020.101880>
- Bonté D, Van Wees JD, Verweij JM (2012) Subsurface temperature of the onshore Netherlands: new temperature dataset and modelling. *Neth J Geosci* 91(4):491–515. <https://doi.org/10.1017/S0016774600000354>
- Bonté D, Smit J, Abdul Fattah RA, Nelskamp S, Cloetingh S, van Wees JD (2020) Quantifying the late-to post-Variscan pervasive heat flow, central Netherlands, Southern Permian Basin. *Mar Pet Geol* 113:104118. <https://doi.org/10.1016/j.marpetgeo.2019.104118>
- Bouroullec RR, Nelskamp S, Loppenburg A, Abdul Fattah R, Foeken J, ten Veen JH (2019) Burial and structural analysis of the dinantian carbonates in the Dutch subsurface. SCAN report. Netherlands Organisation for Applied Scientific Research (TNO); Energie Beheer Nederland B.V. (EBN). https://www.nlog.nl/sites/default/files/2019-09/scan_dinantian_burial_and_structuration_report.pdf. Accessed 14 June 2021
- Bruns B, Di Primio R, Berner U, Littke R (2013) Petroleum system evolution in the inverted Lower Saxony Basin, northwest Germany: a 3D basin modelling study. *Geofluids* 13(2):246–271. <https://doi.org/10.1111/gfl.12016>
- Bruns B, Littke R, Gasparik M, van Wees JD, Nelskamp S (2016) Thermal evolution and shale gas potential estimation of the Wealden and Posidonia Shale in NW-Germany and the Netherlands: a 3D basin modelling study. *Basin Res* 28(1):2–33. <https://doi.org/10.1111/bre.12096>
- Burnham AK, Peters KE, Schenk O (2016) Evolution of vitrinite reflectance models. In: AAPG annual convention & exhibition. AAPG (Calgary, Alberta Canada). June 19–22, 2016
- Collinson JD (2005) Dinantian and Namurian depositional systems in the southern North Sea. In: Collinson JD, Evans D, Holliday D, Jones N (eds) Carboniferous hydrocarbon resources: the southern North Sea and surrounding onshore areas. Yorkshire Geological Society Occasional Publication 7, pp 35–56
- De Gans W (2007) Quaternary. In: Wong TE, Batjes DAJ, de Jager J (eds) Geology of the Netherlands. Royal Netherlands Academy of Arts and Sciences, Amsterdam, pp 173–197
- De Jager J (2003) Inverted basins in the Netherlands, similarities and differences. *Neth J Geosci* 82(4):339–349. <https://doi.org/10.1017/S0016774600020175>
- De Jager J (2007) Geological development. In: Wong TE, Batjes DAJ, de Jager J (eds) Geology of the Netherlands. Royal Netherlands Academy of Arts and Sciences, Amsterdam, pp 5–26
- De Jager J, Geluk MC (2007) Petroleum geology. In: Wong TE, Batjes DAJ, de Jager J (eds) Geology of the Netherlands. Royal Netherlands Academy of Arts and Sciences, Amsterdam, pp 241–264
- Di Primio R, Cramer B, Zwach C, Krooss BM, Littke R (2008) Petroleum systems. In: Littke R, Bayer U, Gajewski D, Nelskamp S (eds) Dynamics of complex intracontinental basins. Springer, Berlin, pp 411–433
- Doornenbal JC, Kombrink H, Bouroullec R, Dalman RAF, De Bruin G, Geel CR, Houben JP, Jaarsma B, Juez-Larré J, Kortekaas M, Mijnlief HF, Nelskamp S, Pharaoh TC, Ten Veen JH, Ter Borgh M, Van Ojik K, Verreussel RMCH, Verweij JM, Vis GJ (2019) New insights on subsurface energy resources in the Southern North Sea Basin area. *Geol Soc Lond Spec Publ*. <https://doi.org/10.1144/SP494-2018-178>
- Duin EJT, Doornenbal JC, Rijkers RHB, Verbeek JW, Wong TE (2006) Subsurface structure of the Netherlands—results of recent onshore and offshore mapping. *Neth J Geosci* 85(4):245–276. <https://doi.org/10.1017/S0016774600023064>
- Ehlers J, Gibbard PL, Hughes PD (2018) Quaternary glaciations and chronology. In: Menzies J, van der Meer JM (eds) Past glacial environments. Elsevier, Amsterdam, pp 77–101
- Froidl F, Zieger L, Mahlstedt N, Littke R (2020a) Comparison of single- and multi-ramp bulk kinetics for a natural maturity series of Westphalian coals: implications for modelling petroleum generation. *Int J Coal Geol* 219:103378. <https://doi.org/10.1016/j.coal.2019.103378>
- Froidl F, Littke R, Baniasad A, Zheng T, Röth J, Böcker J, Hartkopf-Fröder C, Strauss H (2020b) Peculiar Berriasian “Wealden” Shales of northwest Germany: organic facies, depositional environment, thermal maturity and kinetics of petroleum generation. *Mar Pet Geol* 124:104819. <https://doi.org/10.1016/j.marpetgeo.2020.104819>
- Geluk MC (2007) Triassic. In: Wong TE, Batjes DAJ, de Jager J (eds) Geology of the Netherlands. Royal Netherlands Academy of Arts and Sciences, Amsterdam, pp 85–106
- Geluk MC, Paar WA, Fokker PA (2007) Salt. In: Wong TE, Batjes DAJ, de Jager J (eds) Geology of the Netherlands. Royal Netherlands Academy of Arts and Sciences, Amsterdam, pp 283–295
- Geluk M, Grötsch J, Van der Veen H, Van Ojik K (2009) Hydrocarbons in the NE Netherlands—past, present and future. In: 71st EAGE conference and exhibition-workshops and fieldtrips. European Association of Geoscientists & Engineers. <https://doi.org/10.3997/2214-4609.201404948>

- Groetsch J, Sluijk A, Van Ojik K, De Keijzer M, Graaf J, Steenbrink J (2011) The Groningen gas field: fifty years of exploration and production from a Permian dryland reservoir. In: Grötsch J, Gaupp R (eds) *The Permian Rotliegend of the Netherlands*. SEPM special publication 98, Tulsa, Oklahoma, USA, pp 11–33. <https://doi.org/10.2110/pec.11.98.0011>
- Hantschel T, Kauerauf AI (2009) *Fundamentals of basin and petroleum systems modeling*. Springer, Berlin. <https://doi.org/10.1007/978-3-540-72318-9>
- Herngreen GFW, Wong TE (2007) Cretaceous. In: Wong TE, Batjes DAJ, de Jager J (eds) *Geology of the Netherlands*. Royal Netherlands Academy of Arts and Sciences, Amsterdam, pp 127–151
- Hurter S, Haenel R (eds) (2002) *Atlas of geothermal resources in the European Community, Austria and Switzerland*. European Commission, Publ. EUR 17811
- Jasper K, Krooss BM, Flajs G, Hartkopf-Fröder C, Littke R (2009) Characteristics of type III kerogen in coal-bearing strata from the Pennsylvanian (Upper Carboniferous) in the Ruhr Basin, Western Germany: comparison of coals, dispersed organic matter, kerogen concentrates and coal–mineral mixtures. *Int J Coal Geol* 80(1):1–19. <https://doi.org/10.1016/j.coal.2009.07.003>
- Kley J (2018) Timing and spatial patterns of Cretaceous and Cenozoic inversion in the Southern Permian Basin. *Geol Soc Lond Spec Publ* 469(1):19–31. <https://doi.org/10.1144/SP469.12>
- Kley J, Franzke HJ, Jaehne F, Krawczyk C, Lohr T, Reicherter K, Scheck-Wenderoth M, Sipper J, Tanner D, van Gent H (2008) Strain and Stress. In: Littke R, Bayer U, Gajewski D, Nelskamp S (eds) *Dynamics of complex intracontinental basins*. Springer, Berlin, pp 97–124
- Kombrink H (2008) The Carboniferous of the Netherlands and surrounding areas; a basin analysis. *Geologica Ultraiectina* 294. Departement Aardwetenschappen
- Kombrink H, Doornenbal JC, Duin EJT, Den Dulk M, Ten Veen JH, Witmans N (2012) New insights into the geological structure of the Netherlands; results of a detailed mapping project. *Neth J Geosci* 91(4):419–446. <https://doi.org/10.1017/S0016774600000329>
- Krooss BM, Leythaeuser D, Lillack H (1993) Nitrogen-rich natural gases. Qualitative and quantitative aspects of natural gas accumulation in reservoirs. *Erdöl Und Kohle, Erdgas, Petrochemie Vereinigt Mit Brennstoff-Chemie* 46(7–8):271–276
- Krooss BM, Plessen B, Machel HG, Lüders V, Littke R (2008) Origin and distribution of non-hydrocarbon gases. In: Littke R, Bayer U, Gajewski D, Nelskamp S (eds) *Dynamics of complex intracontinental basins*. Springer, Berlin, pp 432–458
- Littke R (1985) Aufbau und Entstehung von Flözen der Dorstener, Horster und Essener Schichten des Ruhrkarbons am Beispiel der Bohrung Wulfener Heide 1. *Bochumer Geol. Geotechn. Arb.* 18
- Littke R, Baker DR, Leythaeuser D, Rullkotter J (1991) Keys to the depositional history of the Posidonia Shale (Toarcian) in the Hills syncline, Northern Germany. In: Tyson RV, Pearson T (eds) *Modern and ancient continental shelf anoxia*. Geological Society Special Publications, vol 58, pp 311–334. <https://doi.org/10.1144/GSL.SP.1991.058.01.20>
- Magri F, Littke R, Rodon S, Bayer U, Urai JL (2008) Temperature fields, petroleum maturation and fluid flow in the vicinity of salt domes. In: Littke R, Bayer U, Gajewski D, Nelskamp S (eds) *Dynamics of complex intracontinental basins*. Springer, Berlin, pp 323–344
- Maystrenko Y, Bayer U, Brink HJ, Littke R (2008) The Central European basin system—an overview. In: Littke R, Bayer U, Gajewski D, Nelskamp S (eds) *Dynamics of complex intracontinental basins*. Springer, Berlin, pp 16–34
- Maystrenko YP, Scheck-Wenderoth M, Anikiev D (2020) 3D-CEBS: three-dimensional lithospheric-scale structural model of the Central European Basin System and adjacent areas. V. 1. GFZ data services. <https://doi.org/10.5880/GFZ.4.5.2020.006>
- McCann T, Pascal C, Timmerman MJ, Krzywiec P, López-Gómez J, Wetzel L, Krawczyk CM, Rieke H, Lamarche J (2006) Post-Variscan (end Carboniferous–Early Permian) basin evolution in western and central Europe. In: Gee DG, Stephenson RA (eds) *European lithosphere dynamics 32*. Geological Society, London, Memoirs, pp 355–388. <https://doi.org/10.1144/GSL.MEM.2006.032.01.22>
- McKenzie D (1978) Some remarks on the development of sedimentary basins. *Earth Planet Sci Lett* 40(1):25–32. [https://doi.org/10.1016/0012-821X\(78\)90071-7](https://doi.org/10.1016/0012-821X(78)90071-7)
- Mijnlieff H, Geluk M (2011) Palaeotopography-governed sediment distribution—a new predictive model for the Permian Upper Rotliegend in the Dutch sector of the Southern Permian Basin. *The Permian Rotliegend of the Netherlands*. SEPM Spec Publ 98:147–159. <https://doi.org/10.2110/pec.11.98.0147>
- Mohnhoff D, Littke R, Sachse VF (2016) Estimates of shale gas contents in the Posidonia Shale and Wealden of the west-central Lower Saxony Basin from high resolution 3D numerical basin modelling. *Zeitschrift Der Deutschen Gesellschaft Für Geowissenschaften* 167:295–314. <https://doi.org/10.1127/zdgg/2016/0053>
- NAM, RGD (1980) Stratigraphic nomenclature of The Netherlands. *Verhandelingen van het Koninklijk Nederlands Geologisch Mijnbouwkundig Genootschap* 32:77
- Nelskamp S (2011) Structural evolution, temperature and maturity of sedimentary rocks in the Netherlands: results of combined structural and thermal 2D modeling. *Fachgruppe für Geowissenschaften und Geographie, Aachen*
- Pepper AS, Corvi PJ (1995) Simple kinetic models of petroleum formation. Part III: modelling an open system. *Mar Pet Geol* 12(4):417–452. [https://doi.org/10.1016/0264-8172\(95\)96904-5](https://doi.org/10.1016/0264-8172(95)96904-5)
- Peters KE, Schenk O, Scheirer AH, Wygrala B, Hantschel T (2017) Basin and petroleum system modeling. In: Hsu CS, Robinson PR (eds) *Springer handbook of petroleum technology*. Springer, Cham, pp 381–417. https://doi.org/10.1007/978-3-319-49347-3_11
- Rawson PF, Riley LA (1982) Latest Jurassic–Early Cretaceous events and the “late Cimmerian unconformity” in North Sea area. *AAPG Bull* 66(12):2628–2648. <https://doi.org/10.1306/03B5AC87-16D1-11D7-8645000102C1865D>
- Rippen D, Littke R, Bruns B, Mahlstedt N (2013) Organic geochemistry and petrography of Lower Cretaceous Wealden black shales of the Lower Saxony Basin: the transition from lacustrine oil shales to gas shales. *Org Geochem* 63:18–36. <https://doi.org/10.1016/j.orggeochem.2013.07.013>
- Rondeel HE, Batjes DAJ, Nieuwenhuijs WH (1996) *Geology of gas and oil under the Netherlands: selection of papers presented at the 1993 international conference of the American Association of Petroleum Geologists, held in The Hague*. Springer, Berlin. <https://doi.org/10.1007/978-94-009-0121-6>
- Sachse VF, Littke R (2018) The impact of Quaternary glaciation on temperature and pore pressure in Jurassic troughs in the Southern Permian Basin, northern Germany. *Geol Soc Lond Spec Publ* 469(1):371–398. <https://doi.org/10.1144/SP469.7>
- Scheck-Wenderoth M, Maystrenko YP (2013) Deep control on shallow heat in sedimentary basins. *Energy Procedia* 40:266–275. <https://doi.org/10.1016/j.egypro.2013.08.031>
- Scheck-Wenderoth M, Maystrenko Y, Hübscher C, Hansen M, Mazur S (2008) Dynamics of salt basins. In: Littke R, Bayer U, Gajewski D, Nelskamp S (eds) *Dynamics of complex intracontinental basins*. Springer, Berlin, pp 307–323
- Scheidt G, Littke R (1989) Comparative organic petrology of inter-layered sandstones, siltstones, mudstones and coals in the Upper Carboniferous Ruhr basin, Northwest-Germany, and their thermal history and methane generation. *Geol Rundschau* 78:375–390

- Schenk O, Peters K, Burnham A (2017). Evaluation of alternatives to Easy% Ro for calibration of basin and petroleum system models. In: 79th EAGE conference and exhibition 2017, vol 2017, no 1, pp 1–5. European Association of Geoscientists & Engineers
- Schroot BM, van Bergen F, Abbink OA, David P, van Eijs R, Veld H (2006) Hydrocarbon potential of the PreWestphalian in the Netherlands on- and offshore—report of the Petroplay project. TNO confidential report - NITG 05-155-C, pp 1–421. <https://www.nlog.nl/sites/default/files/tno%20report-nitg-05-155-c-petroplay.pdf>. Accessed 21 July 2020
- Song J, Littke R, Weniger P, Ostertag-Henning C, Nelskamp S (2015) Shale oil potential and thermal maturity of the Lower Toarcian Posidonia Shale in NW Europe. *Int J Coal Geol* 150:127–153. <https://doi.org/10.1016/j.coal.2015.08.011>
- Song J, Littke R, Weniger P (2017) Organic geochemistry of the lower Toarcian Posidonia shale in NW Europe. *Org Geochem* 106:76–92. <https://doi.org/10.1016/j.orggeochem.2016.10.014>
- Stock AT, Littke R (2018) The Posidonia Shale of northern Germany: unconventional oil and gas potential from high-resolution 3D numerical basin modelling of the cross-junction between the eastern Lower Saxony Basin, Pompeckj Block and Gifhorn Trough. *Geol Soc Lond Spec Publ* 469(1):399–421. <https://doi.org/10.1144/SP469.21>
- Stollhofen H, Bachmann GH, Barnasch J, Bayer U, Beutler G, Franz M, Kästner M, Legler B, Mutterlose J, Radies D (2008) Upper Rotliegend to early cretaceous basin development. In: Littke R, Bayer U, Gajewski D, Nelskamp S (eds) Dynamics of complex intracontinental basins. Springer, Berlin, pp 16–34
- Strozyk F, Urai JL, van Gent H, de Keijzer M, Kukla PA (2014) Regional variations in the structure of the Permian Zechstein 3 intrasalt stringer in the northern Netherlands: 3D seismic interpretation and implications for salt tectonic evolution. *Interpretation* 2(4):101–117. <https://doi.org/10.1190/INT-2014-0037.1>
- Strozyk F, Reuning L, Scheck-Wenderoth M, Tanner DC (2017) The tectonic history of the Zechstein Basin in the Netherlands and Germany. In: Soto JJ, Flinch J, Tari G (eds) Permo-Triassic salt provinces of Europe, North Africa and the Atlantic Margins. Elsevier, Amsterdam, pp 221–241. <https://doi.org/10.1016/B978-0-12-809417-4.00011-2>
- Sweeney JJ, Burnham AK (1990) Evaluation of a simple model of vitrinite reflectance based on chemical kinetics. *AAPG Bull* 74(10):1559–1570. <https://doi.org/10.1306/0C9B251F-1710-11D7-8645000102C1865D>
- Tegelaar EW, Noble RA (1994) Kinetics of hydrocarbon generation as a function of the molecular structure of kerogen as revealed by pyrolysis-gas chromatography. *Org Geochem* 22(3–5):543–574. [https://doi.org/10.1016/0146-6380\(94\)90125-2](https://doi.org/10.1016/0146-6380(94)90125-2)
- TNO-GSN (2020a) DGM-deep V5 on- and offshore, TNO—Geological Survey of the Netherlands. <https://www.nlog.nl/en/dgm-deep-v5-and-offshore>. Accessed 22 July 2020a
- TNO-GSN (2020b) SCAN 2D seismic interpretation and depth conversion for Dinantian, TNO—Geological Survey of the Netherlands. <https://www.nlog.nl/en/scan-2d-seismic-interpretation-and-depth-conversion-dinantian>. Accessed 22 July 2020b
- TNO-GSN (2020c) Stratigraphic nomenclature of the Netherlands, TNO—Geological Survey of the Netherlands. <http://www.dinoloket.nl/en/stratigraphic-nomenclature>. Accessed 19 Sept 2020c
- TNO-NITG, (2004) Geological atlas of the subsurface of the Netherlands—onshore. TNO-NITG, Utrecht, pp 1–104
- Uffmann AK, Littke R (2011) 3D petroleum systems modelling of the North German Basin. *First Break* 29(6):49–63. <https://doi.org/10.3997/1365-2397.2011016>
- Van Adrichem Boogaert HA, Kouwe WFP (1994) Stratigraphic nomenclature of The Netherlands; revision and update by RGD and NOGEP. Mededelingen Rijks Geologische Dienst, vol 50
- Van Buggenum JM, den Hartog Jager DG (2007) Silesian. In: Wong TE, Batjes DAJ, de Jager J (eds) Geology of the Netherlands. Royal Netherlands Academy of Arts and Sciences, Amsterdam, pp 43–62
- Van Balen RT, Van Bergen F, De Leeuw C, Pagnier H, Simmelink H, Van Wees JD, Verweij JM (2000) Modelling the hydrocarbon generation and migration in the West Netherlands Basin, the Netherlands. *Neth J Geosci* 79(1):29–44. <https://doi.org/10.1017/S0016774600021557>
- Van Wees JD, Stephenson RA, Ziegler PA, Bayer U, McCann T, Dadlez R, Gaupp R, Narkiewicz M, Bitzer F, Scheck M (2000) On the origin of the southern Permian Basin, Central Europe. *Mar Pet Geol* 17(1):43–59. [https://doi.org/10.1016/S0264-8172\(99\)00052-5](https://doi.org/10.1016/S0264-8172(99)00052-5)
- Van Wees JD, Van Bergen F, David P, Nepveu M, Beekman F, Cloetingh SAPL, Bonté D (2009) Probabilistic tectonic heat flow modeling for basin maturation: assessment method and applications. *Mar Pet Geol* 26(4):536–551. <https://doi.org/10.1016/j.marpetgeo.2009.01.020>
- Verweij JM (2003) Fluid flow systems analysis on geological time-scales in onshore and offshore Netherlands, with special reference to the Broad Fourteens Basin. Ph.D. thesis, Vrije Universiteit (Amsterdam)
- Verweij HM, Souto Carneiro Echternach M, Witmans N, Abdul Fattah R (2012) Reconstruction of basal heat flow, surface temperature, source rock maturity, and hydrocarbon generation in salt-dominated Dutch Basins, in Peters KE, Curry DJ, Kaciewicz M (eds) Basin modeling: new horizons in research and applications: AAPG Hedberg Series, no 4, pp 175–195. <https://doi.org/10.1306/13311435H43470>
- Warren JK (2008) Salt as sediment in the Central European Basin System as seen from a deep time perspective. In: Littke R, Bayer U, Gajewski D, Nelskamp S (eds) Dynamics of complex intracontinental basins. Springer, Berlin, pp 249–276
- Wehner H, Binot F, Delisle G, Gerling J, Hiltmann W, Kockel F (1989) Genese und Migration von Erdölen im Niedersächsischen Becken: Entwicklung einer integrierten geologisch-geochemischen Explorationsmethoden auf Kohlenwasserstoffe; Abschlussbericht über das westliche Niedersächsische Becken (Raum westlich der Weser). BMFT Forschungsvorhaben, Bundesanstalt für Geowissenschaften und Rohstoffe, Hannover
- Wong TE (2007) Jurassic. In: Wong TE, Batjes DAJ, Jager J (eds) Geology of the Netherlands. Royal Netherlands Academy of Arts and Sciences, Amsterdam, pp 107–126
- Wong TE, de Lugt IR, Kuhlmann G, Overeem I (2007) Tertiary. In: Wong TE, Batjes DAJ, de Jager J (eds) Geology of the Netherlands. Royal Netherlands Academy of Arts and Sciences, Amsterdam, pp 151–173
- Wygrala BP (1989) Integrated study of an oil field in the southern Po basin, northern Italy. *Berichte Kernforschungsanlage Jülich* 2313:1–217
- Ziegs V, Mahlstedt N, Bruns B, Horsfield B (2015) Predicted bulk composition of petroleum generated by Lower Cretaceous Wealden black shales, Lower Saxony Basin, Germany. *Int J Earth Sci* 104(6):1605–1621. <https://doi.org/10.1007/s00531-014-1081-y>